Icarus 318 (2019) 56–74

Contents lists available at ScienceDirect

Icarus

journal homepage: www.elsevier.com/locate/icarus

Ceres' impact craters – Relationships between surface composition and geology

K. Stephan[a,*], R. Jaumann[a,b], F. Zambon[c], F.G. Carrozzo[c], R. Wagner[a], A. Longobardo[c], E. Palomba[c], M.C. De Sanctis[c], F. Tosi[c], E. Ammannito[d], J.-P. Combe[e], L.A. Mc Fadden[f], K. Krohn[a], F. Schulzeck[a], I. von der Gathen[a], D.A. Williams[g], J.E.C. Scully[h], N. Schmedemann[b], A. Neesemann[b], T. Roatsch[a], K.-D. Matz[a], F. Preusker[a], C.A. Raymond[h], C.T. Russell[d]

[a] DLR, Institute of Planetary Research, Berlin, Germany
[b] Free University of Berlin, Germany
[c] INAF-IAPS, Rome, Italy
[d] UCLA, Institute of Geophysics and Planetary Physics, Los Angeles, CA, USA
[e] Bear Fight Institute, Winthrop, WA, USA
[f] NASA Goddard Space Flight Center, Greenbelt, MD, USA
[g] Arizona State University, Tempe, AZ, USA
[h] NASA-JPL Pasadena, CA, USA

ARTICLE INFO

Article history:
Received 27 April 2017
Revised 25 September 2017
Accepted 11 October 2017
Available online 14 November 2017

ABSTRACT

Impact craters of different geological ages, sizes and morphologies are not only the most obvious surface features on Ceres' surface. The investigation of their spectral properties in combination with Ceres' geology and topography reveals not only lateral compositional variations in Ceres' surface material but also possible stratigraphic differences within Ceres' crust. Spectral properties of impact craters with different ages do show distinct trends implying variations with increasing exposure duration of the impact material onto Ceres' surface. Local concentrations of H_2O ice and carbonates are associated with the youngest, either recently emplaced or excavated, surface deposits. On the contrary, regionally higher amounts of ammoniated phyllosilicates originate from deeper regions of Ceres' crust and strengthen the theory of ammonia being a primordial constituent of Ceres. The blue spectral slope, clearly associated with relatively weak absorptions of OH-bearing and/or ammoniated phyllosilicates, is limited to fresh impact material. Either, the blue spectral slope diminishes slowly with increasing geologic age due to space weathering processes, or shortly as a result of gravitation-induced slumping, forming a fine and loosely consolidated regolith.

1. Introduction

For over two years now, three instruments onboard the Dawn spacecraft, the *Framing Camera* (FC) (Sierks et al., 2011), the *Visible and Infrared spectrometer* (VIR) (De Sanctis et al., 2011), and the *Gamma Ray and Neutron Detector* (GRaND) (Prettyman et al., 2011) have been investigating Ceres' geology/topography, its mineralogical and its elemental surface composition, respectively, with unprecedented spatial resolution.

In order to study Ceres' surface in detail a geological mapping campaign has been conducted by the Dawn Science Team resulting in geological maps of Ceres' surface based on imaging data acquired during Dawn's Nominal Mission (March 2015–June 2016) in Ceres' orbit (Williams et al., 2017a). Ceres was divided into 15 regional quadrangles (Roatsch et al., 2016) for which geological maps are available (Williams et al., 2017a). These maps reveal that densely cratered terrain dominates most of Ceres' surface, containing rugged surfaces formed largely by impact structures of all sizes, with a variety of crater morphologies and surface ages. Geomorphological surface features other than impact features identified include: linear structures associated with grooves, pit crater chains, fractures and troughs, of which some are clearly associated with impact craters and others do not appear to have any correlation to an impact event (Buczkowski et al., 2016); and domical features like the peculiar Ahuna Mons (diameter: 20 km, 10.5°S/316.2°E),

* Corresponding author.
E-mail address: Katrin.Stephan@dlr.de (K. Stephan).

https://doi.org/10.1016/j.icarus.2017.10.013
0019-1035/

which have been interpreted as evidence of cryo-volcanic activity on Ceres (Ruesch et al., 2016). The most fascinating geologic feature on the dwarf planet Ceres is the bright material concentrated at the center of impact crater Occator (diameter: 92 km, 19.8°N/239.3°E) suggesting that hydrothermal fluids, driven off by residual impact heat, precipitating solids on the surface and resulted in dome formation in the center (Buczkowski et al., 2017; Schenk et al., 2016).

In addition to the geological maps, the spectral properties of Ceres' surface have been investigated based on FC images and VIR data and the resulting compositional maps are presented in this special issue of Icarus (McCord and Zambon, 2017). The spectral mapping results show that Ceres' surface is mainly composed of phyllosilicates, ammoniated phyllosilicates, carbonates and visually dark opaque probably carbon-rich material (De Sanctis et al., 2015) with the abundance and physical properties, such as grain size, of these compounds varying across Ceres' surface. Local concentration of carbonates (De Sanctis et al., 2016), ammoniated phyllosilicates (Ammannito et al., 2016; Stephan et al., 2017b) and organic material (De Sanctis et al., 2017a) have been identified. Further, local spots, where H_2O ice is exposed on the surface, could be revealed (Combe et al., 2016; Combe et al., 2017; Raponi et al., 2017a).

In order to understand the processes responsible for the formation and exposition of these compounds and their implications for Ceres' geological history, we combined the results of the geological and spectral mapping campaigns to assess general and local relationships between composition and geology. We study the variations in the spectral properties of Ceres with respect to their association to specific surface features as well as their geographic and topographic location. Because impact craters are the most ubiquitous Cerean surface feature, our focus lies in the investigation of the spectral properties of Ceres' impact craters. Depending on their dimensions, the individual impact events probe different depths of Ceres' crust. Thus, differences in the spectral properties of these impact craters could not only reveal lateral heterogeneities in the composition of Ceres' crust but also point to a possible spatial variability in the relative mineral abundance in a stratified upper crustal layer. Further, surface ages derived by the Dawn Science team during the geological mapping campaign enable to put the mapped spectral properties of these impact craters into a temporal context. Fresh impact crater material generally reflects un-weathered composition of Ceres' crust, but possibly also reveals modifications in the chemical and/or physical properties of the surface material caused by the impact process itself. Finally, depending on the specific crater age, i.e. how long the impact material has been exposed on Ceres' surface, space weathering effects (bombardment by micro-meteorites, solar wind particles and cosmic rays) that change the spectral properties with time might be revealed.

2. Data basis and methodology

The Dawn mission has mapped Ceres during the *High Altitude Mapping Orbit* (HAMO) phase and *Low Altitude Mapping Orbit* (LAMO) phase from an altitude of about 1950 and 850 km, respectively (Russell et al., 2016). Images of the Framing Camera reach spatial resolutions up to ~140 m/pixel (HAMO) and ~35 m/pixel (LAMO). The spatial resolution of individual VIR observations ranges between ~ 360 m per pixel during HAMO and ~90 m per pixel during LAMO, which enables the mapping of local spatial variations in Ceres' surface composition.

FC clear filter images offer the geological context information for our study, including the surface ages as derived by measurements of crater size frequency distributions (Hiesinger et al., 2016; Schmedemann et al., 2016). Absolute ages of Cerean impact craters, which are essential to determine the accurate timescales of Ceres' evolution, have been derived during the Dawn geological mapping campaign (Williams et al., 2017a) based on the two chronology systems outlined in Hiesinger et al. (2016), i.e. the LDM (*lunar-derived model*) and the ADM (*asteroid-derived model*). In addition, FC clear filter images have been used to produce a stereophotogrammetric-based *digital terrain model* (DTM) derived from HAMO data (135 m/pixel) (Preusker et al., 2016), enabling the investigation of spectral properties and their relationship to the surface topography.

Images acquired in the seven band pass filters of the FC camera also provide multispectral information at the highest spatial resolution available. These filters are sensitive at 440 nm (filter 8), 550 nm (filter 2), 650 nm (filter 7), 750 nm (filter 3), 830 nm (filter 6), 920 nm (filter 4), and 965 nm (filter 5). Whereas these images do not offer a continuous spectrum like the VIR observations, they are useful for seeing spatial variations in the visible albedo and spectral slope at a much higher spatial resolution. FC color composites derived for images of filters 5, 2 and 8 as well as ratio images of filters 8 and 3 have been found to highlight most spectral variations identified on Ceres (Pieters et al., 2016).

The study of global relationships between composition and geology is based on global photometrically corrected mosaics of Ceres separately produced for images acquired during the HAMO phase with the clear filter, as well as with the 7 color filters of the FC instrument (Roatsch et al., 2016). The clear-filter map is shown in Fig. 1a with the corresponding color-coded HAMO DTM in Fig. 1b. Figs. 1c and 2a show the global maps derived for an enhanced true color mosaic, combining the mosaics derived from images of filters 5, 2 and 8, and a classification of the spectral slope derived from the ratio of the FC images taken in the filters 8 and 3, respectively. Ratio values lower than one indicate a positive (red) spectral slope and ratio values higher than one imply a negative (blue) spectral slope. In order to distinguish a spectrally-derived slope from a terrain's topographic slope, in the following, we use the term red or blue spectral slope to describe the variations in the FC derived ratio values measured across Ceres' surface. For local comparisons we additionally used individual FC clear filter images acquired during the LAMO phase, preferentially images acquired at a similar time as the corresponding VIR observation of the area of interest, i.e. exhibiting similar illumination conditions.

The spectral investigation of Ceres' surface using VIR data described in detail by Ammannito et al. (2016), Carrozzo et al. (2016) and Ciarniello et al. (2016) has been performed by measuring specific spectral parameters, for example the wavelength position and depths of individual absorptions, which are related to a particular surface compound. The depths of the absorptions at 2.7 and 3.1 µm, which occur in every VIR spectrum of Ceres, indicate the existence and variation in the abundance and/or grain size of OH-bearing and ammoniated minerals (Ammannito et al., 2016; Stephan et al., 2017a). Global maps showing the variations in these two spectral parameters have been produced by the VIR team (Fig. 2b and c). These VIR derived maps have proven to be useful in revealing global differences in Ceres' chemical/physical surface properties both laterally and potentially also with crustal depth and allow to put the color variations observed in the FC images into compositional context. Spectral parameter maps of type localities discussed in this study were produced from individual VIR observations. Because strong absorptions at 3.4 and 3.9 µm are only apparent in local areas enriched in carbonates, their depths have been calculated only for specific areas of interest. In order to avoid misinterpreting the VIR spectra due to temperature effects, a correction of the thermal signal in the 3- to 5-micron region has been performed following the procedure of Raponi et al. (2017a).

Whereas FC as well as VIR data allow the investigation of Ceres' entire surface, difficult illumination conditions in the polar regions make a detailed comparison between results of different data sets

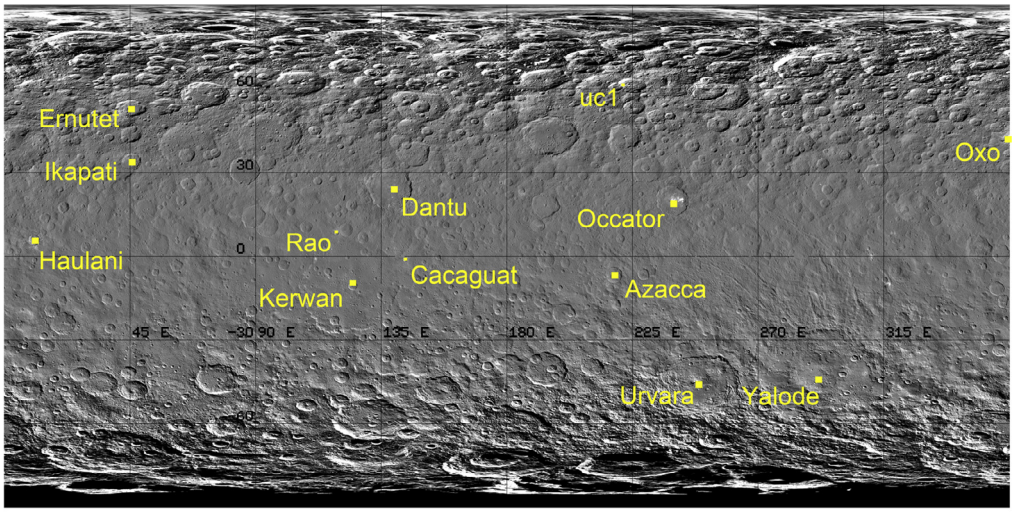

a

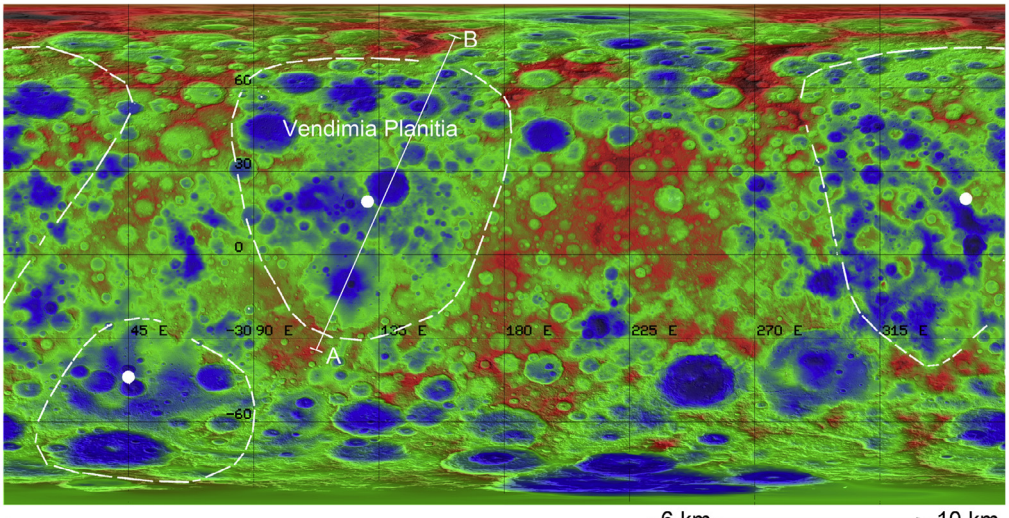

b

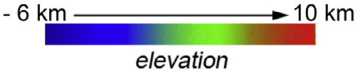

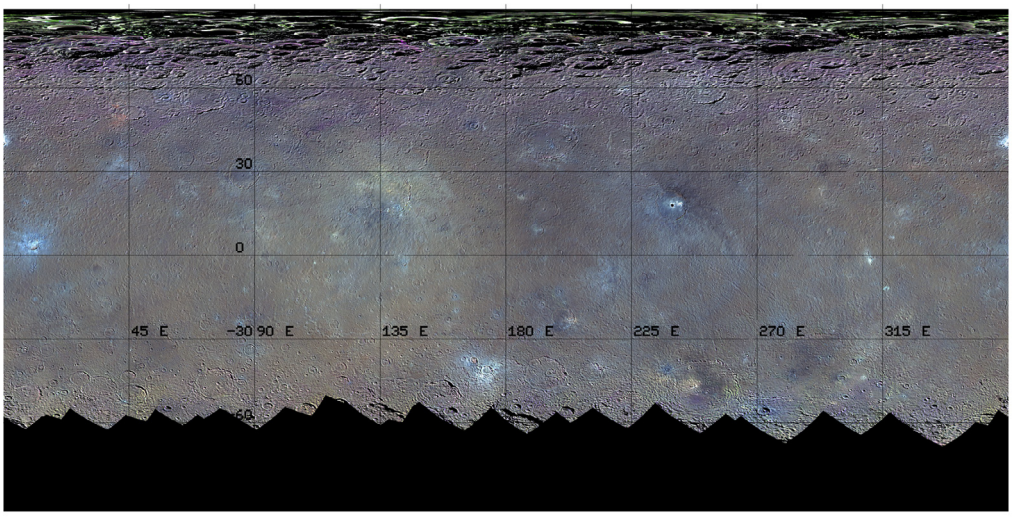

c

R: 956nm (F5) G: 555nm (F2) B: 440 nm (F8)

Fig. 1. Global views of Ceres' surface based on HAMO data of the FC instrument: a) clear filter mosaic with the mentioned impact craters highlighted, b) the FC-derived DTM produced by Preusker et al. (2016) including the location (extension and center) of large degraded impact basins identified by Marchi et al. (2016) and of the topographic profile shown in Fig. 3, and c) the FC color composite mosaic (produced by K.D. Matz / DLR).

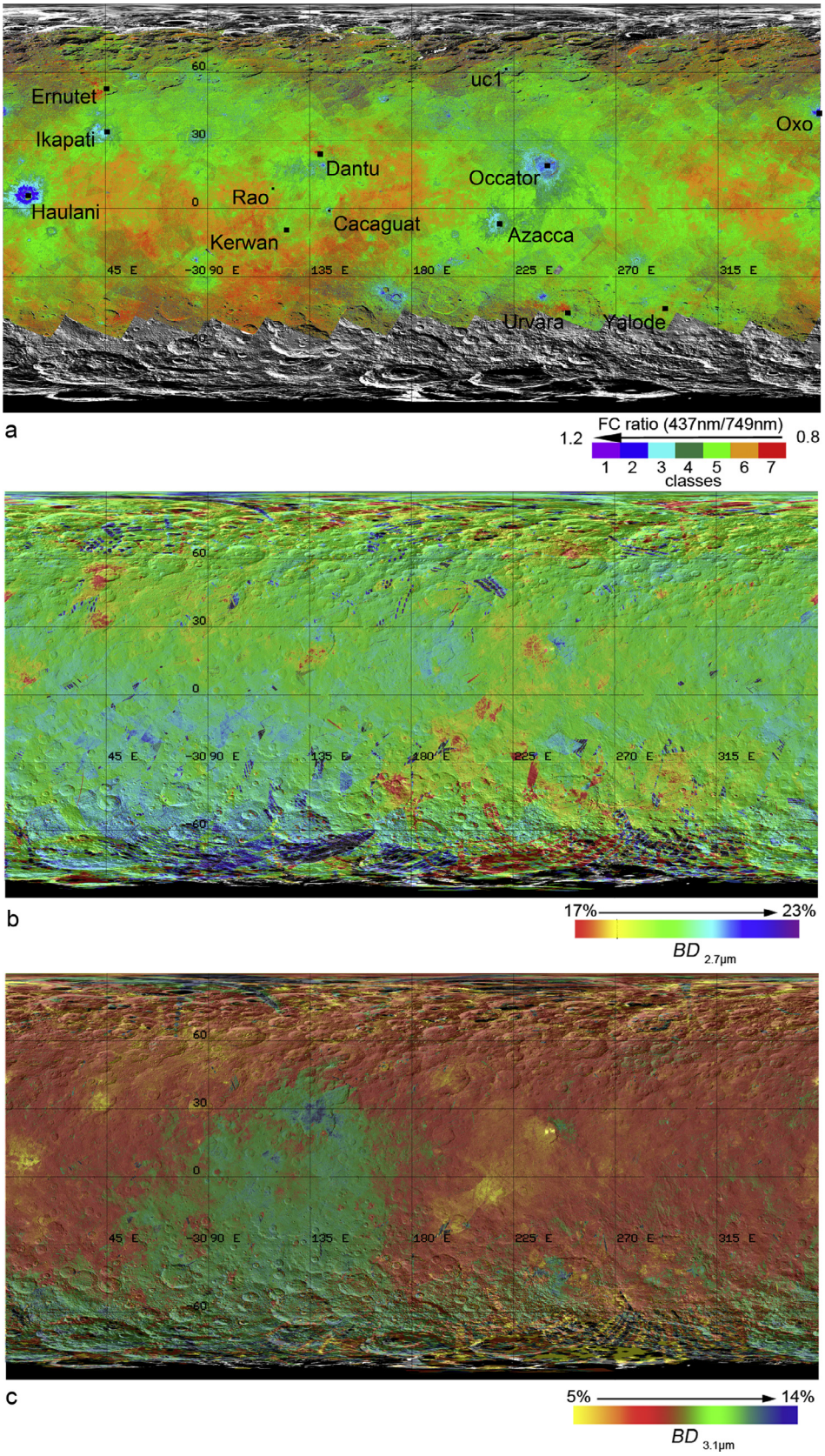

Fig. 2. Global views of Ceres surface based on HAMO data from the FC and VIR instrument: a) FC-derived slope classification map (adapted from Stephan et al., 2017a), b) and c) the VIR-derived variations in the *band depth* (BD) of the two major absorptions at 2.7 and 3.1 µm indicative of OH-bearing and ammoniated minerals, respectively.

challenging. Therefore, we concentrate the investigation of individual impact features on Ceres' surface on a local scale, which are situated in regions between 60°N and 60°S. In order to relate the VIR results to Ceres' geology and topography, we use the precise geometric correction and registration of the VIR-derived spectral parameter maps to corresponding FC maps and images. This is essential for avoiding misinterpretation in case of local differences in the surface composition.

3. General relationships between spectral properties and geological units

The global geologic map of Ceres as presented in Buczkowski et al. (2016) and Mest et al. (2017) shows that densely cratered terrain forms most of Ceres' surface. Only on a regional scale is it superimposed and ejecta-blanketed by the 280-km large impact crater Kerwan (10.8°S/124°E) and the Urvara/Yalode crater system (Mest et al., 2017), i.e. impact materials of the impact craters Urvara (diameter: 170 km; 46.6°S/249.2°E and Yalode (diameter: 260 km; 42.6°S/292.5°E) that cover extended parts of Ceres' eastern and southern hemisphere (Mest et al., 2017). Impact craters are the most ubiquitous geomorphic features on Ceres (Buczkowski et al., 2016) (Fig. 1a) and appears in a wide range of sizes, morphologies and degree of degradation. Intriguingly, impact craters larger than 300 km are absent. However, DTMs of Ceres' surface (Fig. 1b) show broad expanses of low-lying terrains and only small areas of elevated terrain with an overall relief of about 16 km (Hiesinger et al., 2016; Jaumann et al., 2016). The low-lying terrains could represent the remnants of old, completely degraded impact basins (Marchi et al., 2016), whereas the topographic heights within the elevated areas appear to be composed of large knobs and the rims of moderately sized craters (Mest et al., 2017; Williams et al., 2017b).

Based on stratigraphic horizons, such as the globally effective Kerwan, Yalode and Urvara impact events, a time stratigraphic system of Ceres has been established by the Dawn team (Mest et al., 2017; Wagner et al., 2016; Williams et al., 2017a). The system starts with the *Pre-Kerwanan*, the oldest chronologic period (>2.4 Ga / ADM, >2.5 Ga / LDM; Pasckert et al., 2017), followed by the *Kerwanan* (>165±25 Ma / ADM; >695±155 Ma / LDM; Pasckert et al., 2017), the *Yalodean* (>37.5±18.5 Ma / ADM; >135±45 Ma / LDM; Pasckert et al., 2017 and Crown et al., 2017) and the *Urvaran* (>46±5 Ma / ADM; >76±10 Ma / LDM; Crown et al., 2017 and Schmedemann et al., 2016). The youngest period of the *Azaccan* ('Era of rayed craters') has been defined based on the impact crater Azacca (diameter: 49.9 km, 6.7°S/218.4°E). Azacca is the oldest impact crater (45.8±5 Ma /ADM; 75.9±10 Ma / LDM) on Ceres' surface that still exhibits a distinct ray system, which is the major characteristic of a morphologically fresh impact crater (Melosh, 1989).

At a first glance, global maps of Ceres' spectral properties derived from FC and VIR data (Figs. 1c and 2) do not show any immediately noticeable relationship with the geologic units defined by Mest et al. (2017). The FC maps (Fig 1a and c) and the classification map derived from the ratio of the FC filter images centered at 437 nm (F8) and 749 nm (F3) (Fig. 2a) show only a few small, high-albedo (>9%), bluish colored areas with a blue spectra slope (FC slope class 1–3), which are associated with prominent impact craters such as for instance Occator, Haulani (diameter: 34 km, 5.8°N/10.8°E), and Oxo (diameter: 10 km, 42.2°N/359.6°E). The remaining areas exhibit a reddish color and a rather red spectral slope, the typical appearance of Ceres' geologically old densely cratered terrain. The VIR derived BD map of the absorption at 2.7 µm shows a similar pattern (Fig. 2b) with relative low BD values (~17%) associated to the blue-sloped impact craters (FC slope classes 1–3) and relatively high BD values between ~20 and ~23% in the red-sloped areas (FC slope classes 5–7).

An exception to the typical global spectral trends occurs in Ceres's eastern hemisphere, where a higher visible albedo feature (Fig. 1a and c) apparently correlates with an extended area of a stronger 3.1 µm-absorption (Fig. 2c) with BDs of up to ~14%. This feature could be associated with Vendimia Planitia, a ~800 km large depression possibly representing remnants of one of the ancient impact basins postulated by Marchi et al. (2016) and reach southward to the southern polar region. Whereas the latter could be influenced by photometric effects due to unfavorable illumination, the deep absorptions in the area of Vendimia Planitia could imply a regional increase in the abundance of ammonium-bearing phyllosilicates in Ceres' crust also identified by Marchi et al. (2016) and De Sanctis et al. (2017b). Either these heterogeneities occur laterally across Ceres' surface or indicate a higher abundance of ammonium-bearing phyllosilicates in deeper regions of Ceres' crust.

The fact that this relationship is most pronounced in Vendimia Planitia could be explained by the superimposed prominent and geologically younger 284 and 126 km large impact craters Kerwan (1300±160 / LDM and 281±17 / ADM; Schmedemann et al., 2016 and Williams et al., 2017b) and *Dantu* (24.3°N/138.2°E; ~70–150 Ma, Kneissl et al., 2016), respectively (see Section 3.2). Fig. 3 combines the topographic profile across the region of Vendimia Planitia with the measured FC ratio classes as well as the variations in the BD values of the absorptions at 2.7 and 3.1 µm. The distribution of the FC-derived ratio classes, which indicate a rather neutral (neither red nor blue) spectral slope throughout the area, does not show any correlation with the ancient impact basin or Dantu and Kerwan. Instead, the BD values of the absorptions at 2.7 and 3.1 µm are strongest near Dantu, which is located approximately in the center of Vendimia Planitia, and close to Kerwan.

Dantu is the youngest of these three impact features. Its ejecta are expected to cover large portions of Kerwan, whose ejecta probably cover most of the remaining area of Vendimia Planitia. Nevertheless, the material excavated by the Vendimia impact event probably represents deep subsurface material, which originates from and thus provides a view into the composition of Ceres' deeper crust. Given, Dantu's and Kerwan's location inside of Vendimia Planita, implies that both impacts without any doubt re-excavated material related to the Vendimia Planitia event and probed into much greater depths of Ceres crust, than similarly large impact craters outside of this ancient huge impact basin. The impact events which created this candidate basin could have excavated and distributed material from a maximum depth of ~40–50 km, assuming that the maximum depth of excavation is approximately 1/10 of the transient crater diameter (Melosh, 2011). The transient crater diameters of the presumed Vendimia basin, Kerwan and Dantu are retrieved from several crater scaling laws (Hiesinger et al., 2016; Melosh, 2011; Zahnle et al., 2003), based on a simple-to-complex transition diameter of 10 km for Ceres (Hiesinger et al., 2016). Depending which formula for the calculation of the transient crater diameter is used, these diameters range from ~420–480 km for the presumed Vendimia basin, ~165–190 km for Kerwan, and ~80–95 km for Dantu, corresponding to depths of excavation of ~40–50 km, ~17–19 km, and ~8–9 km, respectively.

In the Dantu impact event no subsurface levels considerably deeper than ~10 km could have been reached but the Dantu impactor as well as the Kerwan impactor most likely have probed into material originating from depths ~40–50 km distributed in the Vendimia event. Models of the interior structure of Ceres assume that an outer about 70–190 km thick volatile-rich layer composed of carbonates or phyllosilicates, H_2O ice, and salts and/or clathrate hydrates overlies a denser interior of hydrated silicates (Ermakov

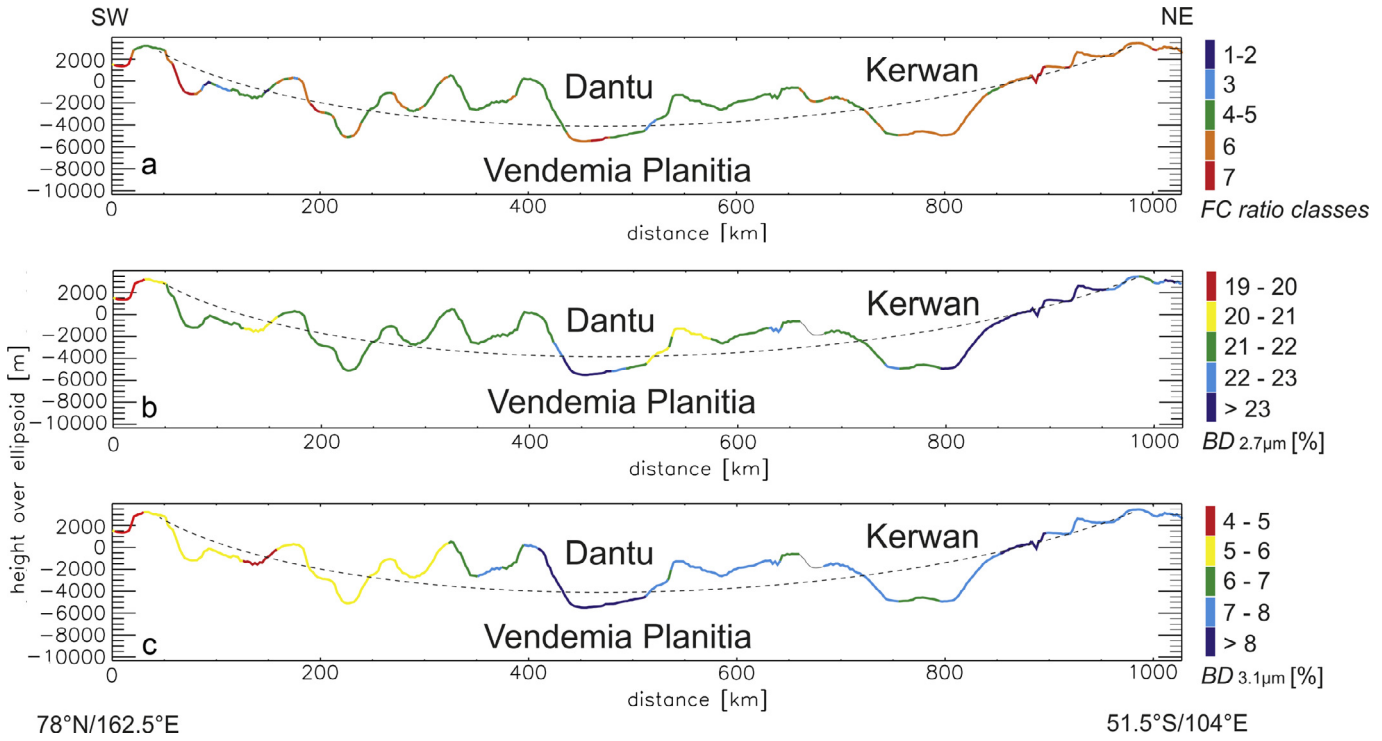

Fig. 3. Topographic profiles across Vendimia Planitia (located as shown in Fig. 1b) including superimposed impact craters such as Dantu and Kerwan colored with respect to a) the FC ratio classes, as well as the local BDs of Ceres' two major absorptions b) at 2.7 and c) at 3.1 µm. The dotted line indicates the estimated topographic profile of Vendimia Planitia as derived from low-pass filtering of the DTM (Marchi et al., 2016).

et al., 2017; Fu et al., 2017; Park et al., 2016; Raymond et al., 2017). The Vendimia impact event could have punched through the crust and could even have reached this denser interior, distributing material enriched in ammonium-bearing phyllosilicates on the surface. Material from the greatest depths to be reached in an impact event is deposited close to the crater in the continuous ejecta and/or is part of the crater floor material (Melosh, 2011). This could explain the strong phyllosilicate signature in Dantu (Stephan et al., 2017b), which is located approximately in the center of the presumed Vendimia impact structure.

Impact processes are the most dominant geologic process on planetary surfaces and therefore it is not surprising that obviously variations in the spectral properties of Ceres' surface are directly associated with impact craters. However, as seen in the global maps of Figs. 1 and 2, not every impact crater on Ceres exhibits an equally unique spectral signature. In addition to compositional differences with increasing crustal depth, differences in the spectral properties could be expected due to the impact process itself. Schmedemann et al. (2016) and Stephan et al. (2017a) already pointed out that only morphologically fresh impact craters and their ejecta deposits are characterized by a bluish color and blue spectral slope, which could be directly related to differences in the physical and/or chemical properties of the surface material by processes expected to happen during an impact process (such as brecciation, grinding, and melting). In addition, depending how long the crater and ejecta material has been exposed on the surface, their spectral properties could reflect alterations in the physical and/or chemical properties of the surface material with time due to the space weathering effects such as (micro-)meteoritic impacts, solar wind, exposure to void with loss of volatiles, diurnal and/or seasonal variations of the surface temperature.

In order to further improve our understanding of the relationships between the spectral properties of impact craters and any differences in the surface composition due to the impact process and/or weathering as well as compositional differences within Ceres' crust, we additionally investigated the spectral properties of impact craters on Ceres' surface mapped by VIR and FC on a local scale in comparison to 1) the geologic context, including the association of spectral properties with specific (inter) crater features, 2) as a function of the corresponding crater model age, as well depending on 3) the local topographic level / stratigraphic location. All impact craters, for which crater model ages have been measured during the Dawn geologic mapping campaign (Williams et al., 2017a) have been investigated, and the results presented in the next sections depending on the chronology of their emplacement on Ceres' surface.

3.1. Geologically old Yalodean and Kerwanan impact craters and basins

The largest oldest impact features on Ceres' surface still visible in the FC clear filter images are large impact basins such as Kerwan (~1.3 Ga /LDM, ~281 Ma /ADM, Williams et al., 2017b) and Yalode (~ 1.1 Ga / LDM, Crown et al., 2017). These basins usually exhibit a highly degraded morphology and a discontinuous, partly polygonal rim, as shown for Yalode in Fig. 4. Nevertheless, their ejecta deposits extend for more than a hundred kilometer into the surrounding heavily cratered terrain. Smooth material filling the basin floors has been interpreted as impact-induced melt derived from volatile-enriched crustal material (Crown et al., 2017; Williams et al., 2017b). Some of their interiors contain an irregular ring of low hills that could represent a basin inner ring (Crown et al., 2017).

FC color variations and VIR- derived spectral differences in the vicinity of these impact basins could be only identified, where geologically younger surface features such as small impact craters superimpose these basins (see Section 3.3). The spectral properties associated to the basins themselves cannot be distinguished from their surrounding regions (Fig. 4). Rather, they are included

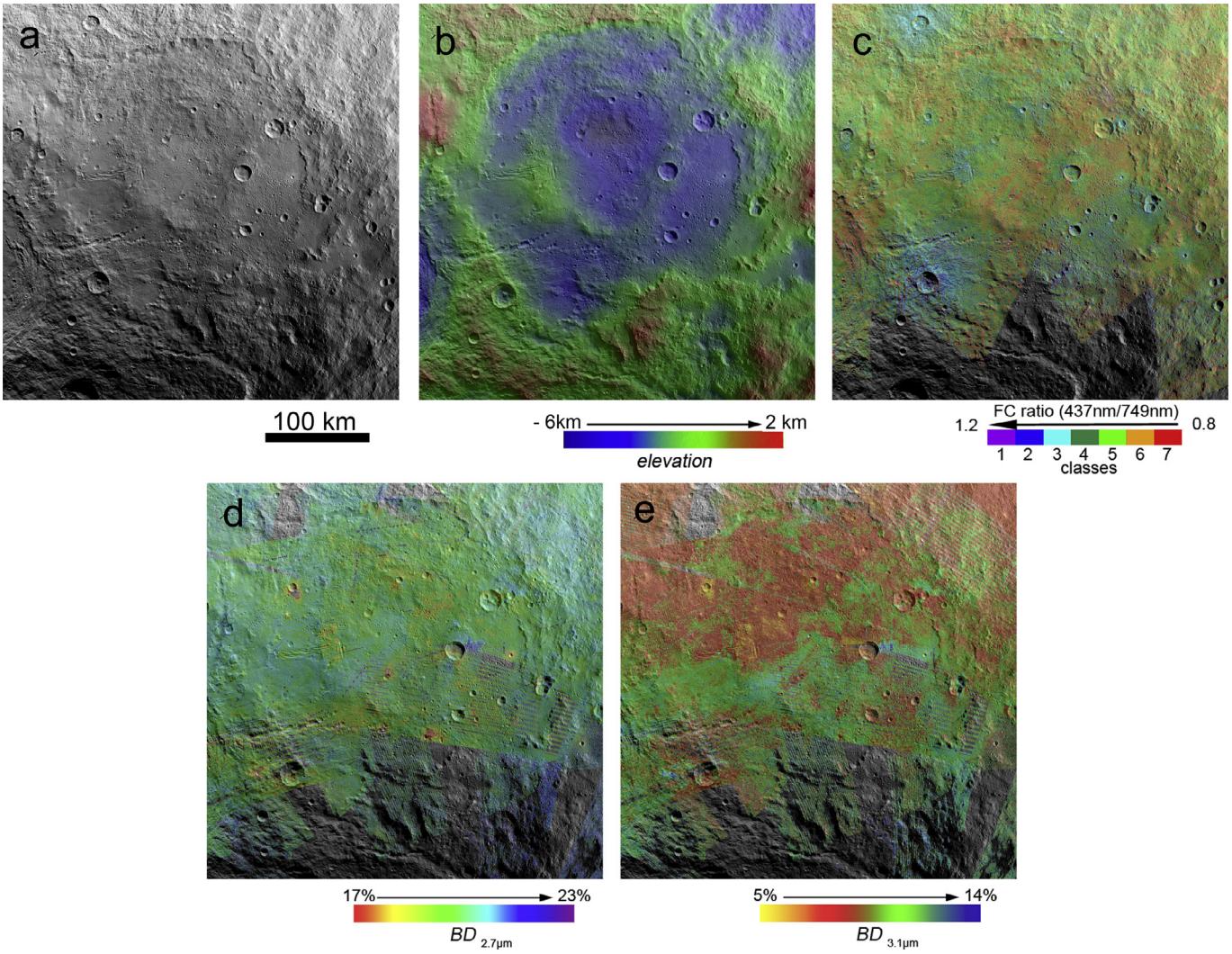

Fig. 4. Impact basin Yalode as seen by a) the FC Clear filter in comparison with b) the corresponding DTM, c) the FC slope/ratio classes as well as the band depths (*BD*) of absorptions at d) 2.7 and e) 3.1 µm.

in the spectral units of Ceres' heavily cratered and weathered terrain characterized by a reddish/brownish color with a red spectral slope and a VIR spectrum similar to the average spectrum of Ceres (De Sanctis et al., 2015). This is likely caused by hundreds of millions of years of space weathering including impact gardening and gravity-driven mass wasting (Fig. 4). Thus, after a period of about 1 billion years of exposing the basin material to the space environment (impacting micro-meteorites, solar wind particles and cosmic rays) an equalization of the spectral properties of the basin materials and the cratered terrain was reached.

Nevertheless, a few presumably geologically old localities could be observed on Ceres' surface, which do not follow this trend. In particular, the 930±230 Ma-old (Wagner et al., 2016) impact crater Ernutet (diameter: 53.4 km; 52.9°N/45.5°E) in Ceres' northern hemisphere partly exhibits an unusual steep red spectral slope (Fig. 5c), as can already be seen in the global FC ratio classification map in Fig. 2a. In contrast, the phyllosilicate absorption at 2.7 µm is quite weak (BD of ~17%) (Fig. 5d), which is usually the case in the vicinity of fresh impact craters (see Section 3.3) (Stephan et al., 2017a), whereas the absorption at 3.1 µm exhibits an intermediate strength (~10%) in this area (Fig. 5e). In the vicinity of Ernutet, however, additional absorptions at 3.4 and 3.9 µm, associated with carbonates, have been identified (De Sanctis et al., 2017a; Raponi et al., 2017b). The absorption at 3.4 µm, however, could also be caused by organic material i.e. aliphatic compounds exposed on Ceres' surface (De Sanctis et al., 2017a), which normally exhibit a red spectral slope.

The spectrally distinctive region is located in the southern portion and the western crater wall of Ernutet and extends across its crater rim, which might indicate an association of the concentration in carbonates or organic-rich material with Ernutet's ejecta deposits. The spectrally red-sloped signature is strongest in the southern portion of Ernutet, where the impact crater overlaps an old strongly degraded impact crater with a size similar to that of Ernutet (Fig. 5). In addition, Ernutet lies in a topographic depression, suggesting that the described spectral variations might indicate compositional heterogeneities in the sub-surface material of this region. However, taking the spectral properties of similarly old impact craters into account and the local appearance of possibly organic material (De Sanctis et al., 2017a), an exogenic origin of the organic material (impactor material) independently of the Ernutet impact event cannot be excluded at this point.

3.2. Large mid-aged Urvaran impact craters

Relatively large (>100 km) mid-aged impact craters such as Urvara (~134 Ma; Schmedemann et al., 2016, Fig. 6) and Dantu (Fig. 7) have been interpreted as a major marker in Ceres' geologi-

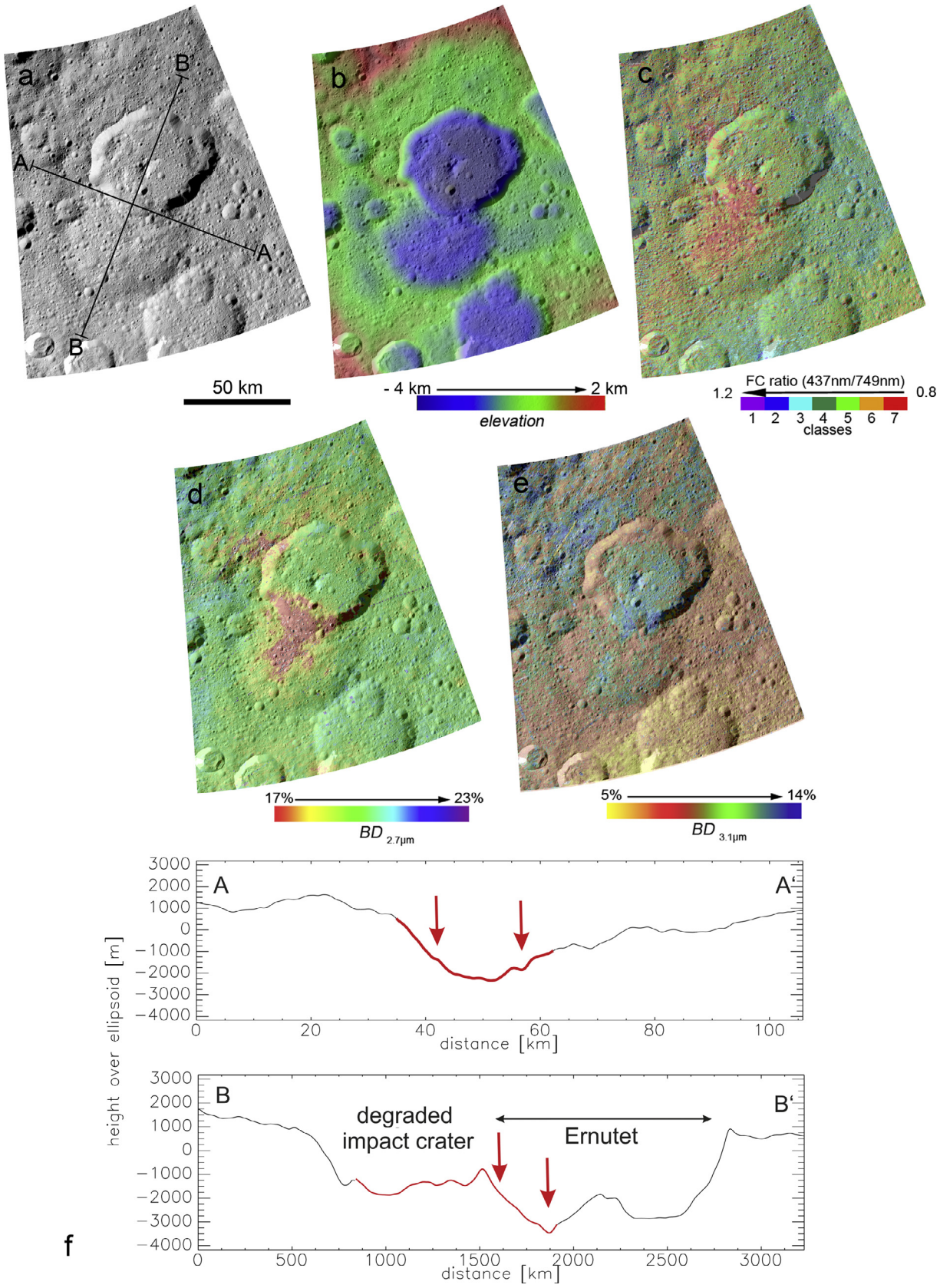

Fig. 5. Impact crater Ernutet as seen by (a) the FC Clear filter in comparison with the corresponding (b) HAMO DTM, (c) the FC slope/ratio classes, the BDs of the absorptions at (d) 2.7 and (e) 3.1 µm as well as (f) the topographic profiles as indicated in (a) the clear filter image with the location of the red-sloped material highlighted by the red-colored portion of the profile. Arrows point to the location of the reddest spectral slope in the area of Ernutet. (For interpretation of the references to color in this figure legend, the reader is referred to the web version of this article.)

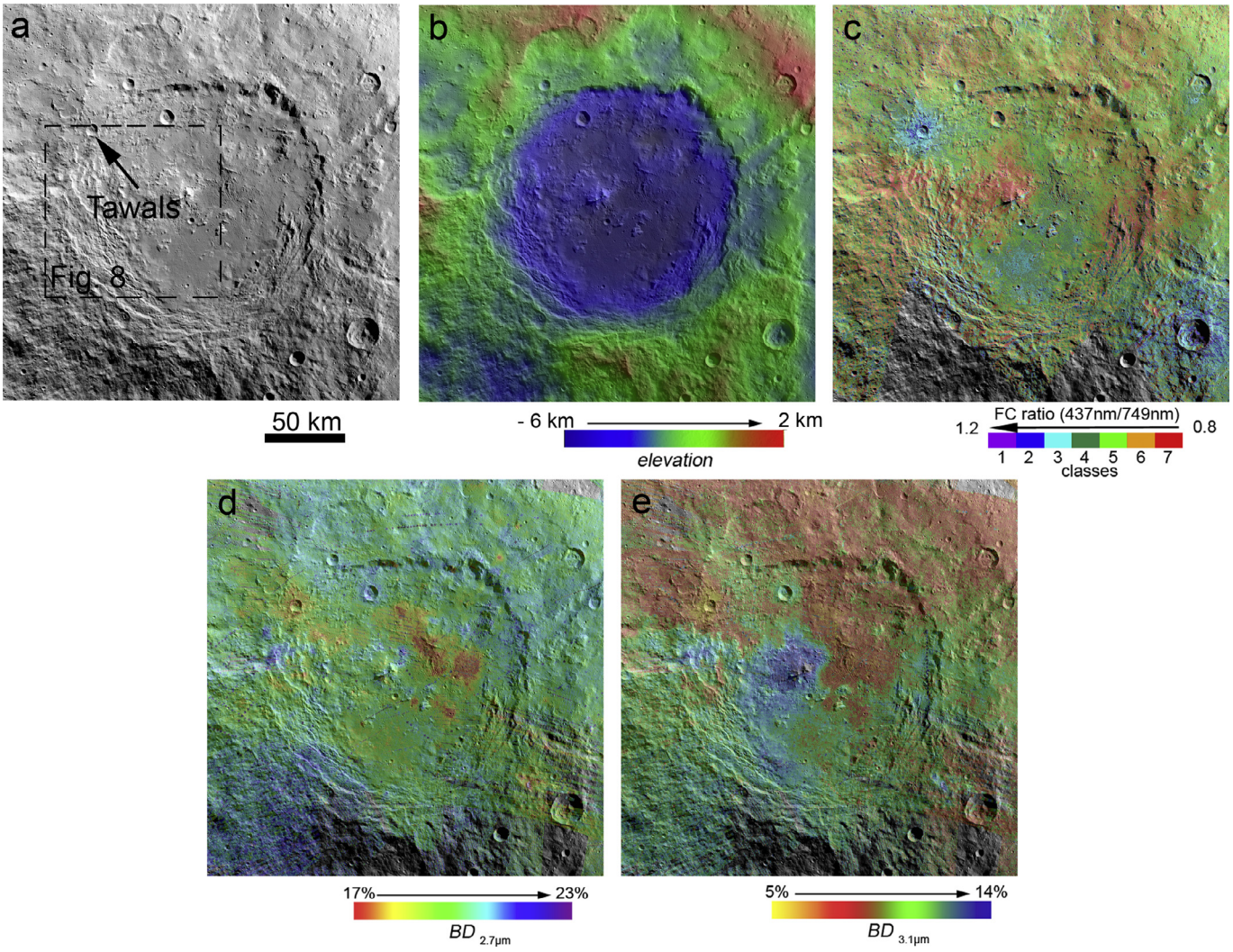

Fig. 6. Impact crater Urvara as seen by a) the FC Clear filter in comparison to b) the corresponding DTM, c) the FC slope/ratio classes as well as the BDs of the absorptions at d) 2.7 and e) 3.1 µm. The black box indicates the close-up image in Fig. 8 (e–h). The black arrow indicates to location of the small fresh superimposed impact crater Tawals (see Section 3.3).

cal evolution following the Yalodean era (Mest et al., 2017). These impact features not only still show well preserved and complex crater morphologies and extended ejecta blankets, but also a complex surface composition associated with intra-crater features.

In comparison to Yalode, the DTMs of Urvara and Dantu exhibit sharply defined continuous crater rims. Nevertheless, both impact features show a distinct crater modification with partly collapsed crater walls and material slumped into the crater covering the crater floor. Complex craters such as Urvara and Dantu exhibit central peaks similar to the central peak of the geologically younger impact features of Occator (Buczkowski et al., 2017). In the case of older impact craters such as Urvara and Dantu, however, central peaks are frequently collapsed in such a way that the only remaining indication of the peaks appear as sets of morphologic ridges. For example, the central area of Urvara is characterized by a 20-km long east-west trending ridge. Dantu exhibits a central pitted area enclosed by a disconnected ring of ridges, which has been interpreted by Williams et al. (2017b) as the remnants of a collapsed central peak.

As described above, Dantu lies completely within an extended region of relatively deep phyllosilicate absorptions at 2.7 and 3.1 µm, implying a higher abundance of ammoniated phyllosilicates (Stephan et al., 2017b), that might be associated with the formation of the ancient impact basin Vendimia Planitia (Marchi et al., 2016) (Fig. 2b and c). The deepest phyllosilicate absorptions measured in this region and anywhere on Ceres (Ammannito et al., 2016) occur in Dantu's pitted central area (Figs. 7 and 8a–d), which has been interpreted as the remnants of a collapsed central peak. Central peaks are thought to be composed of crustal material uplifted during the latter stages of the impact event. This crustal material commonly originates from the deeper portions of the crustal material below the crater floor that became excavated during the impact (Cahill et al., 2009; Melosh, 1989; Wieczorek and Zuber, 2001). As demonstrated above, in case of Dantu this would mean that crustal material from a depth of about 8–9 km could make up the central peak's material, which furthermore lies in the center of the underlying impact basin of Vendimia Planitia. Thus, the concentration of ammoniated phyllosilicates in Dantu's central peak material similar to the one in the entire region of Vendimia Planita supports the theory that an increasing amount of ammoniated phyllosilicates occurs with increasing depth of Ceres' crust. A similar assumption could be adopted as explanation for the local deepening of the 3.1µm-absorption (BD ~14%) near Urvara's central peak (Ammannito et al., 2017) (Figs. 6 and 8e–h). Although, Urvara lies in a topographically higher region than Dantu, the corresponding DTM (Fig. 6b) shows that the Urvara impact event still

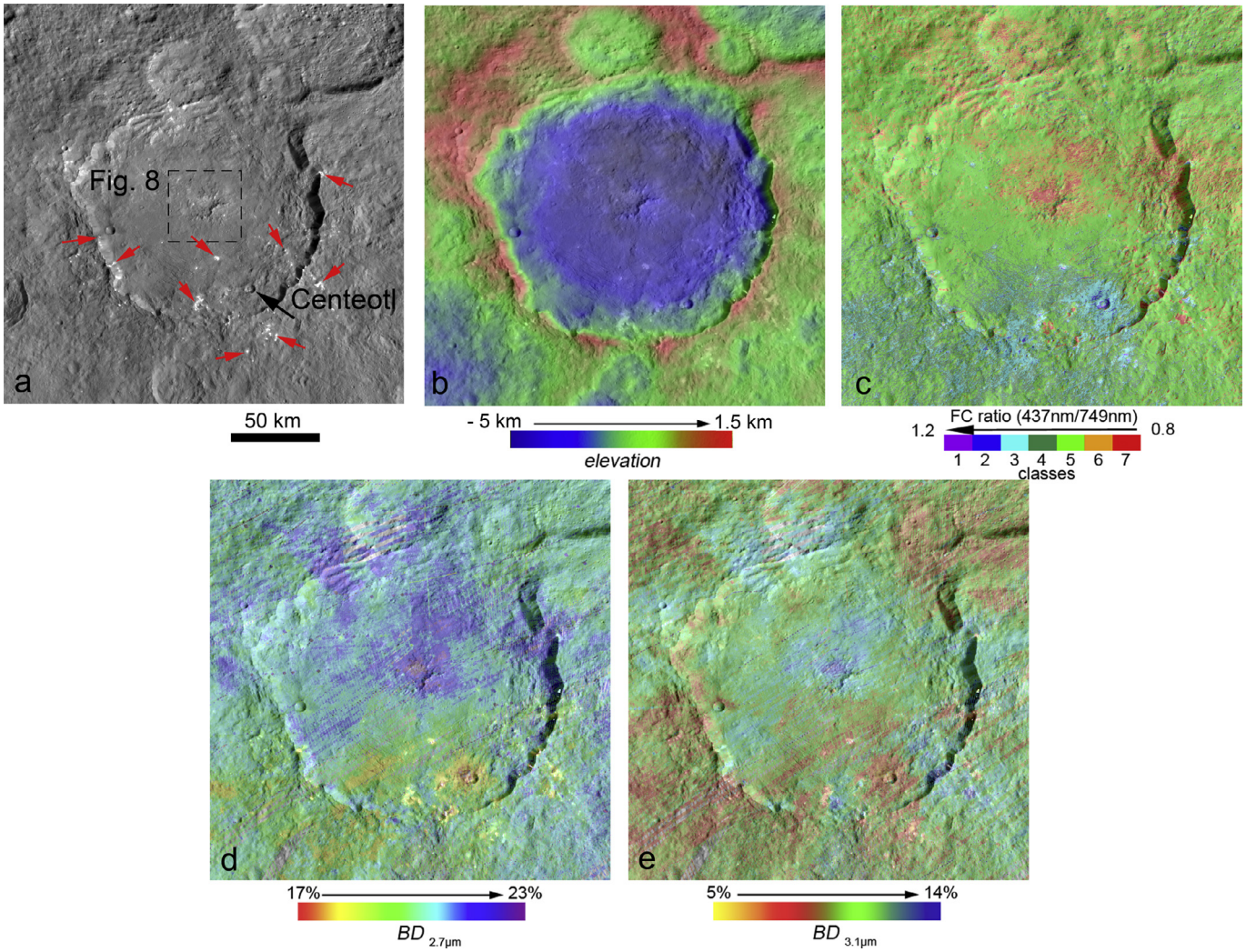

Fig. 7. Impact crater Dantu as seen by the FC Clear filter in comparison to the corresponding DTM, the FC slope/ratio classes as well as the BDs of the absorptions at 2.7 and 3.1 µm. The black box indicates the close-up image in Fig. 8 (a–d). The black arrow points to the small fresh impact crater Centeotl superimposed on Dantu's floor, and the red arrows point to bright spots enriched in carbonates (see Section 3.3). (For interpretation of the references to color in this figure legend, the reader is referred to the web version of this article.)

probed Ceres' crust at a considerable crustal depth (~6 km) and that at least Urvara's central peak could reach the ammonium-enriched region in the deeper Cerean crust. Nevertheless, the concentration of ammonium-bearing compounds in a deeper crustal region would strengthen the theory that ammonia is a primordial constituent of Ceres. Either accreted as organic matter or as ice, it may have reacted with phyllosilicates during Ceres' differentiation (De Sanctis et al., 2015).

Although most parts of Dantu's ejecta show a neutral spectral slope, this central pitted area of Dantu is characterized by a distinct red spectral slope (Fig. 7c) – similar to the red-sloped material in the center of Urvara (Ammannito et al., 2017; Stephan et al., 2017b) (Fig. 6c). These areas corresponds to other spectrally red-sloped surface areas, which are covered with material emplaced by landsides along the crater walls, such as seen in portions of Urvara's western crater wall (Fig. 8e–h), and possibly remobilized terrace materials.

Sets of fractures covering portions of Urvara's and Dantu's crater floor often show a spectral signature similar to neighboring small fresh impact craters, such as Tawals (diameter: 8.8 km; 39.1°S/238.0°E; Fig. 6) located at the northwestern rim of Urvara (Ammannito et al., 2017; Stephan et al., 2017a) and Centeotl (diameter: 6 km; 18.9°N/141.2°E; 4.2±3 / LDM and 6.7±4 / ADM; Wagner et al., 2017; Fig. 7) in the southern portion of Dantu's floor (Palomba et al., 2017a). Although these floor fractures probably have been be formed during Dantu's crater modification (Melosh, 1989), they could have been reactivated in younger times due to Centeotl's and Tawals' impact events and expose fresh surface material. The spectral characteristics of fresh crater material as well as the bright spots on the southern portion of Dantu's floor and ejecta blanket (their locations are indicated by the red arrows in Fig. 7), which represents the youngest surface deposits on Ceres, are presented in the following section.

3.3. Small and mid-sized fresh Azaccan impact craters (< 80 Ma)

One of the most intriguing type of the Cerean impact craters are the morphologically fresh ones, i.e., those emplaced during the geological era of the Azaccan (younger than ~80 Ma old) (Schmedemann et al., 2016). Their crater material presumably reflects the more or less un-weathered surface composition of Ceres' crust or the modified result of the impact event. All impact craters of this group show pristine morphologies with sharp and relatively steep crater walls, well-defined ejecta deposits (blankets/rays), as well as only a few superimposed impact craters on their crater floor and ejecta blankets (Schmedemann et al., 2016). Sizes of fresh

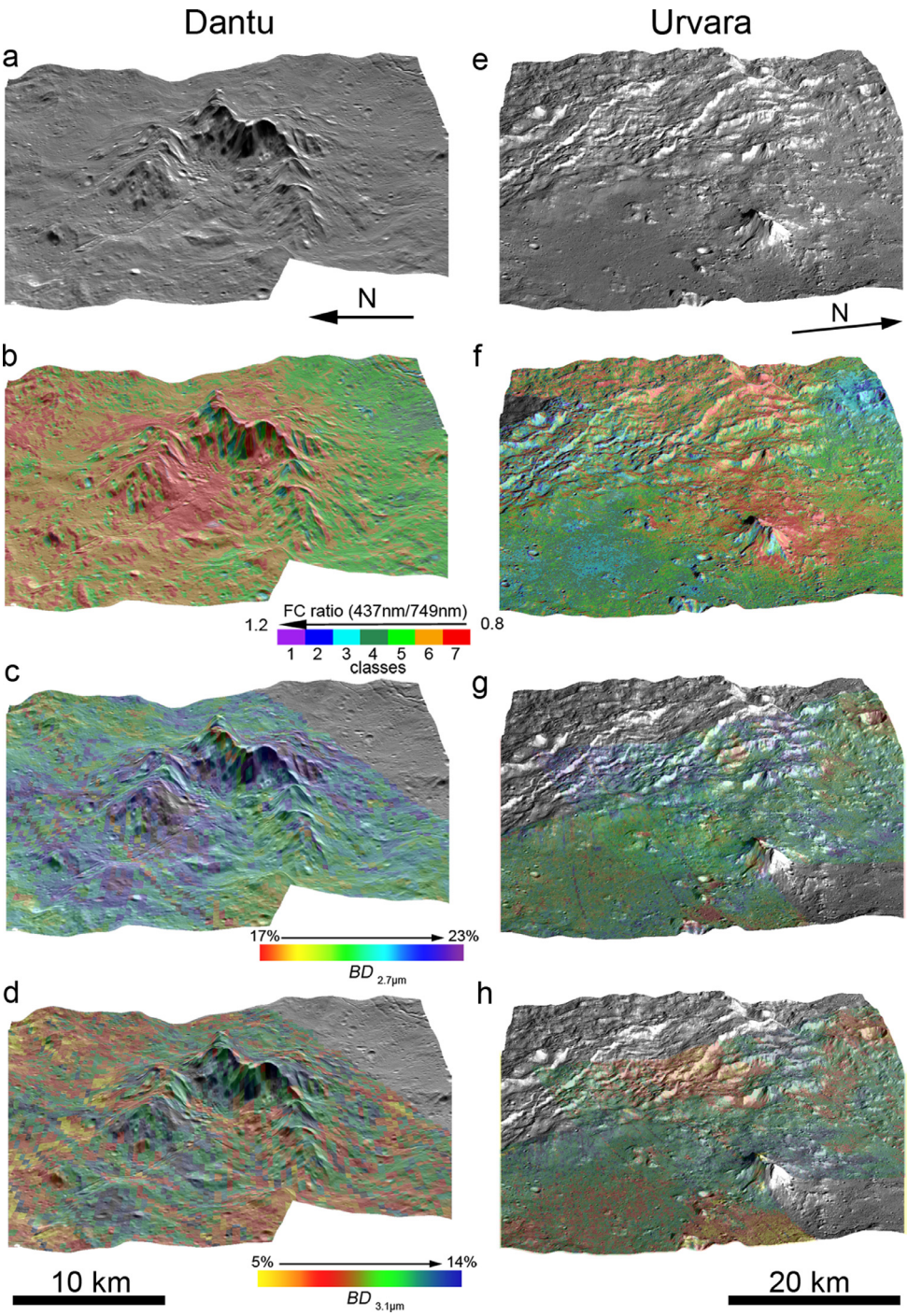

Fig. 8. 3D views of Dantu's central peak area in comparison to Urvara's central area, including Urvara's western collapsed crater wall as seen by the FC Clear filter (a, e), the FC slope/ratio classes (b, f) as well as in the VIR-derived BD maps of the absorptions at 2.7 (c, g) and 3.1 µm (d, h). The locations of both local areas with respect to Urvara and Dantu are indictated in Figs. 6 and 7, respectively.

impact craters on Ceres vary from a few kilometers up to ~100 km. Small fresh impact craters show the typical bowl-shaped morphology. Larger, more complex craters such as Occator (Buczkowski et al., 2016; Russell et al., 2016) sometimes show specific intra-crater features (central peaks). Depending on the local topography, portions of their crater walls may have collapsed with material from the surrounding region slumping into the crater (Buczkowski et al., 2016; Krohn et al., 2017).

The major spectral characteristics of Ceres' fresh impact craters are a blue spectral slope and relatively weak phyllosilicate absorptions at 2.7 and 3.1 µm (Stephan et al., 2017a). The oldest examples of this crater group are Azacca (~80Ma, Schmedemann et al., 2016) and Ikapati (diameter: 50 km; 33.8°N/45.6°E; ~45 Ma, Schmedemann et al., 2016). In contrast to the overall rather reddish/brownish looking surface of Ceres, both impact craters show a slightly blue spectral slope (Figs. 9 and 10). The blue spectral slope is mostly associated with morphologically smooth plains on their crater floor and ejecta blanket that have been interpreted as impact melt (Krohn et al., 2016). The material forming these plains extends from the crater interior into topographic depressions covering the pre-existing surface. Krohn et al. (2016) showed that Ikapati has been emplaced in a terrain of a relatively steep topo-

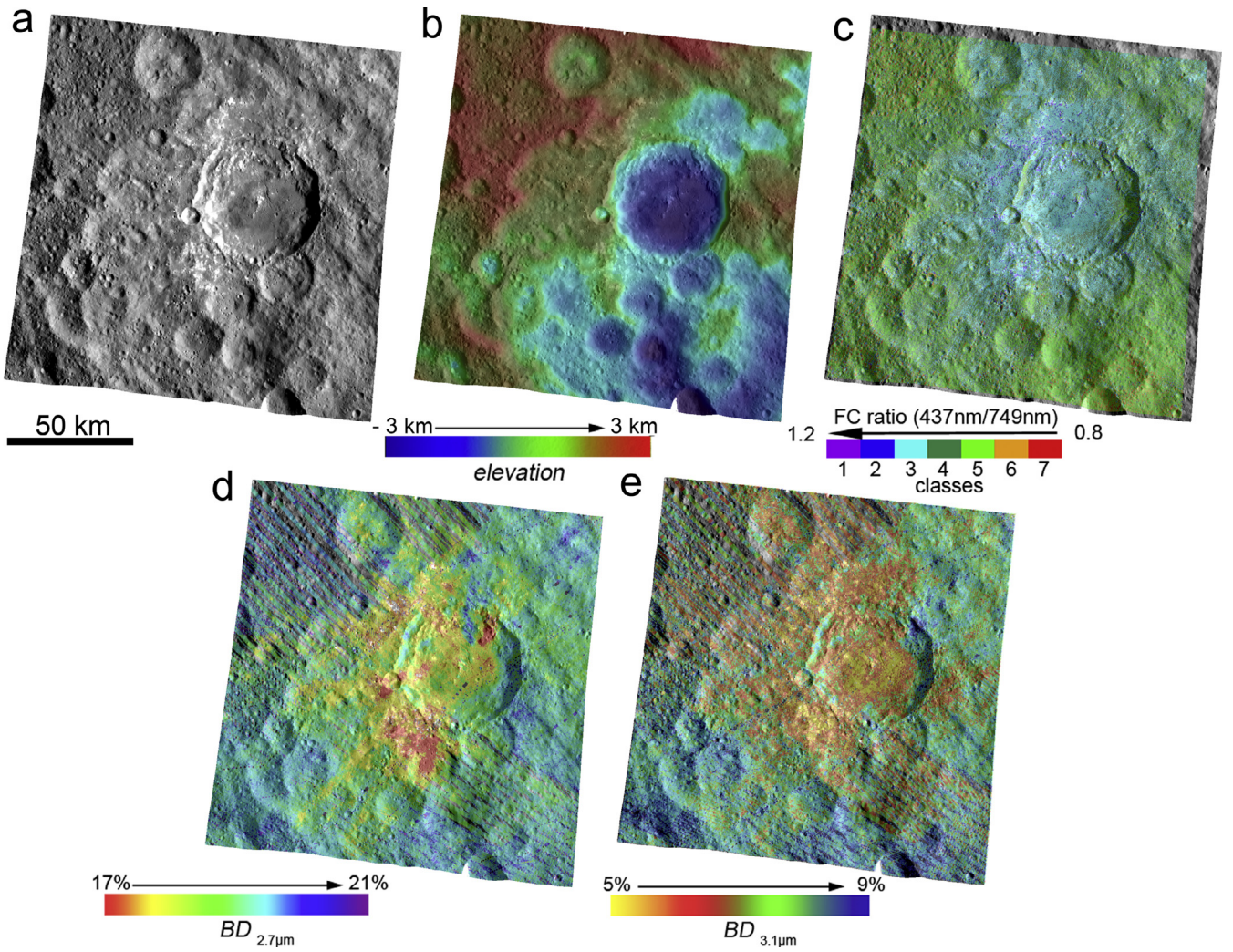

Fig. 9. Impact crater Azacca as seen by (a) the LAMO FC Clear filter image f2_497507088 in comparison to (b) the corresponding DTM, and (c) the FC slope/ratio classes as well as the BDs of the absorptions at (d) 2.7 and (e) 3.1 µm.

graphic slope, explaining the asymmetric distribution of the bluish material. The blue spectral slope correlates clearly with relatively weak phyllosilicate absorptions at 2.7 and 3.1 µm, indicating a different composition and/or physical properties of the phyllosilicates than the surrounding old cratered terrain (Ammannito et al., 2016; Stephan et al., 2017a).

Nevertheless, younger impact craters also differ in their spectral properties with respect to each other. Many of the youngest impact craters on Ceres exhibit a relatively high visible albedo, such as Haulani (diameter: 34 km; ~2 Ma (Schmedemann et al., 2016); 5.8°N/10.8°E), which is presented in detail in Krohn et al. (2017) and Tosi et al. (2017). Some morphologically fresh and spectrally blue-sloped craters, however, do not. Thus, the two small impact craters Tawals and Centeotl exhibit a slightly lower visible albedo than their surroundings in the corresponding FC images. Tawals is located at the margin of the impact basin Urvara (Fig. 6) and Centeotl can be found in the southern portion of impact crater Dantu (Fig. 7). The dark albedo of these impact craters could indicate compositional differences compared to the other fresh spectrally blue-sloped craters. The lower albedo could be explained by a higher contribution of carbon-rich material, which is spectrally featureless in the wavelength range detected by VIR. Either it represents a possible remnant of the impactor material or became excavated from Ceres' subsurface.

Few impact craters, such as Oxo (diameter: 10 km; 0.5 Ma (Schmedemann et al., 2016); 42.2N°/359.6E°), which is discussed in detail by Combe et al. (2016), additionally exhibit some evidence of H_2O ice at their crater walls. Oxo is located in a topographic depression (~ 3 - 4 km below the reference surface of the DTM), on the rim of an older impact crater. Because Dawn's GRaND instrument (Prettyman et al., 2017) predicts extensive amounts of H_2O ice hidden in Ceres' subsurface, the icy material could have been excavated as a result of the impact event forming Oxo. Local deposits of H_2O ice could also be detected in the vicinity of the small impact crater Kahukura (diameter: 6.3 km, 61.4°N/221.4°E) (Fig. 11). Kahukura lies in a topographically much higher position (< 1 km below Ceres' reference surface of the DTM) than Oxo (~ - 4 km, Combe et al., 2016). Furthermore, the icy deposits are detectable only close to and possibly extend into the shadowed region of the crater floor (Fig. 12). Thus, taking into account the location of Kahukura close to Ceres' northern polar region, the H_2O ice on its floor rather represent icy material trapped in a relatively cold, nearly-permanently shadowed area (Platz et al., 2016).

Intriguingly, Kahukura also shows a distinct carbonate signature with prominent absorptions at 3.4 and 3.9 µm (De Sanctis et al., 2016) on its crater walls (Figs. 11 and 12). Regions enriched in carbonates were first identified in the bright spots of impact crater Occator, named Cerealia and Vinalia Faculae (De Sanctis et al.,

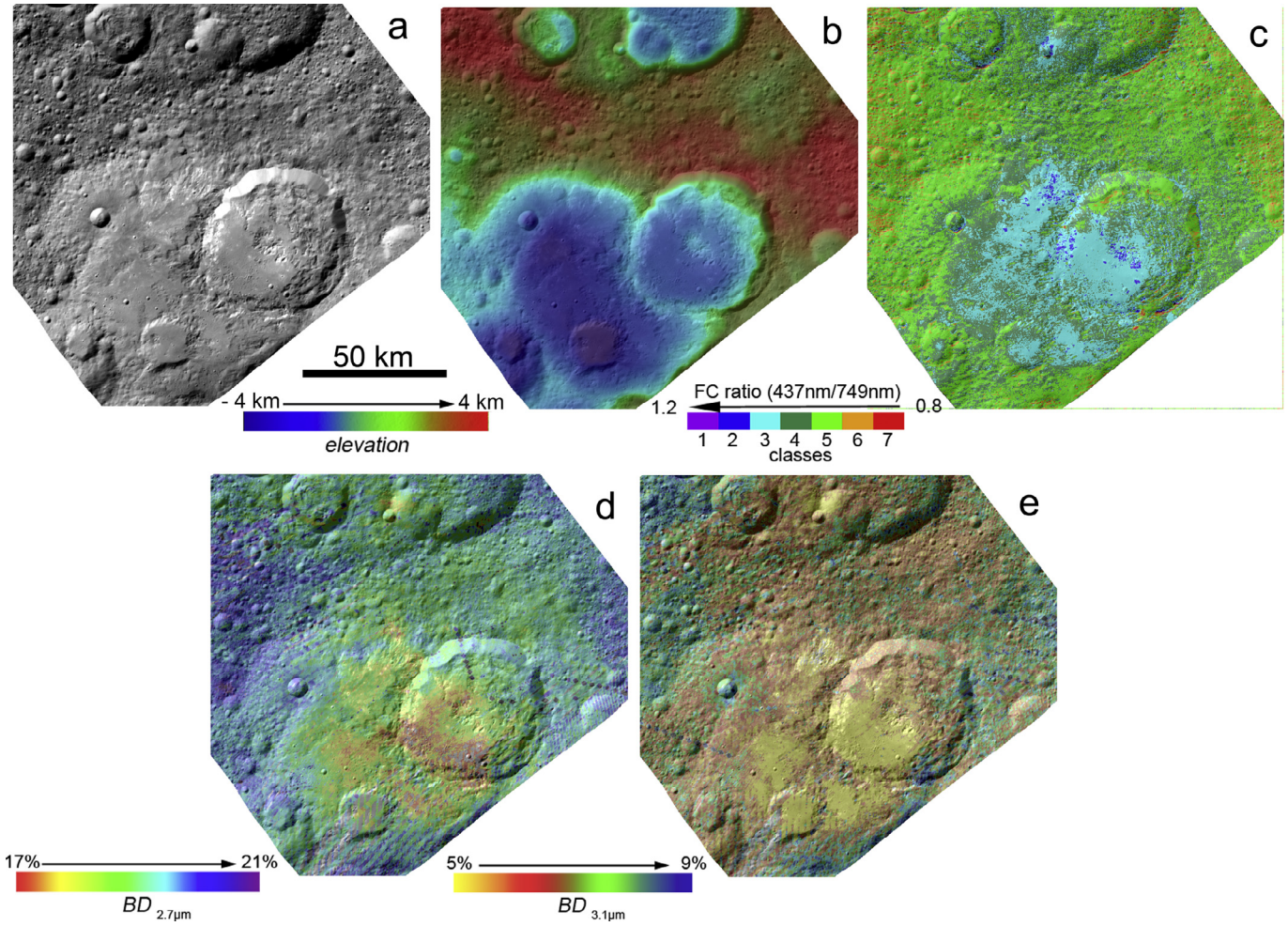

Fig. 10. Impact crater Ikapati as seen by (a) the LAMO FC Clear filter in comparison to (b) the corresponding DTM, (c) the FC slope/ratio classes as well as the BDs of the absorptions at (d) 2.7 and (e) 3.1 µm.

2016). Recently, numerous bright spots enriched in carbonates were identified on Ceres's surface. Their spectral properties and association with geological/geomorphological surface features have been discussed in detail by Palomba et al. (2017b). Carbonate-rich areas generally show weak phyllosilicate absorptions at 2.7 and 3.1 µm, similar to the spectrally blue-sloped fresh impact craters discussed here. Cerealia and Vinalia Faculae, the bright spots in the vicinity of Dantu and in impact crater Kupalo are characterized by the highest concentration of carbonates observed on Ceres. The corresponding VIR spectra exhibit a slight shift of the 2.7 µm absorption towards longer wavelengths (De Sanctis et al., 2017b; Palomba et al., 2017b; Stephan et al., 2017b). The shift has been interpreted as differences in the actual composition of the phyllosilicates with more Al-bearing than Mg-bearing phyllosilicates (De Sanctis et al., 2016) or by the spectral signature of the carbonates, or hydration (Palomba et al., 2017b).

Bright deposits enriched in carbonates on Ceres are mostly associated with morphologically fresh surface features. The bright spots of Occator have been interpreted as possible more or less recently deposited post-impact fluids (De Sanctis et al., 2016) or impact-triggered outgassing (Schenk et al., 2016; Zolotov, 2017). The same could be valid for Dantu, where a few of the bright spots appear closely related to inner-crater fractures on Dantu's floor. On the contrary, in case of Kahukura an excavation of carbonate-rich material from the subsurface is more likely the cause (Fig. 11).

Even more, regions, where fresh carbonate-enriched deposits dominate, sometimes exhibit a red spectral slope. A few bright spots near Dantu (Fig. 7) as well as the Cerealia and Vinalia Faculae (Longobardo et al., 2017) exhibit a F8/F3 ratio value smaller than 0.8, which implies an even redder spectral slope than measured for the old cratered terrain (F8/F3 ratio value >0.8 - 0.9). A red spectral slope, however, has been also observed in case of the collapsed central peaks and crater walls of Dantu and Urvara (Figs. 6 and 7) and unconsolidated slumping material such as in case of the impact crater Juling (diameter: 20 km, 35.9°S/218.4°E) (De Sanctis et al., 2017b) (Fig. 13). The crater walls and ejecta of Juling as well as of its neighboring impact crater Kupalo (diameter: 26 km; 6.7°S/218.4°E] exhibit the typical spectral characteristics of a fresh Cerean impact crater with a blue spectral slope and weak phyllosilicate absorptions (Stephan et al., 2017a). In contrast to Kupalo, however, the material covering Juling's crater floor exhibits a spectrally red-sloped signature (Fig. 13). In the case of Juling the red spectral slope is likely indicating slumping material transported from the northern topographic heights into the topographic depression, where Juling is located (Stephan et al., 2017a). Conversely, Kupalo is situated topographically relative high with high-standing crater walls shield the crater from a similar fate.

Thus, in contrast to a blue spectral slope, which apparently characterizes specifically physical properties, a red spectral slope in the Ceres' spectra apparently indicates either a different mineralogy as in case of Ernutet (when strong absorptions at 3.4 µm is

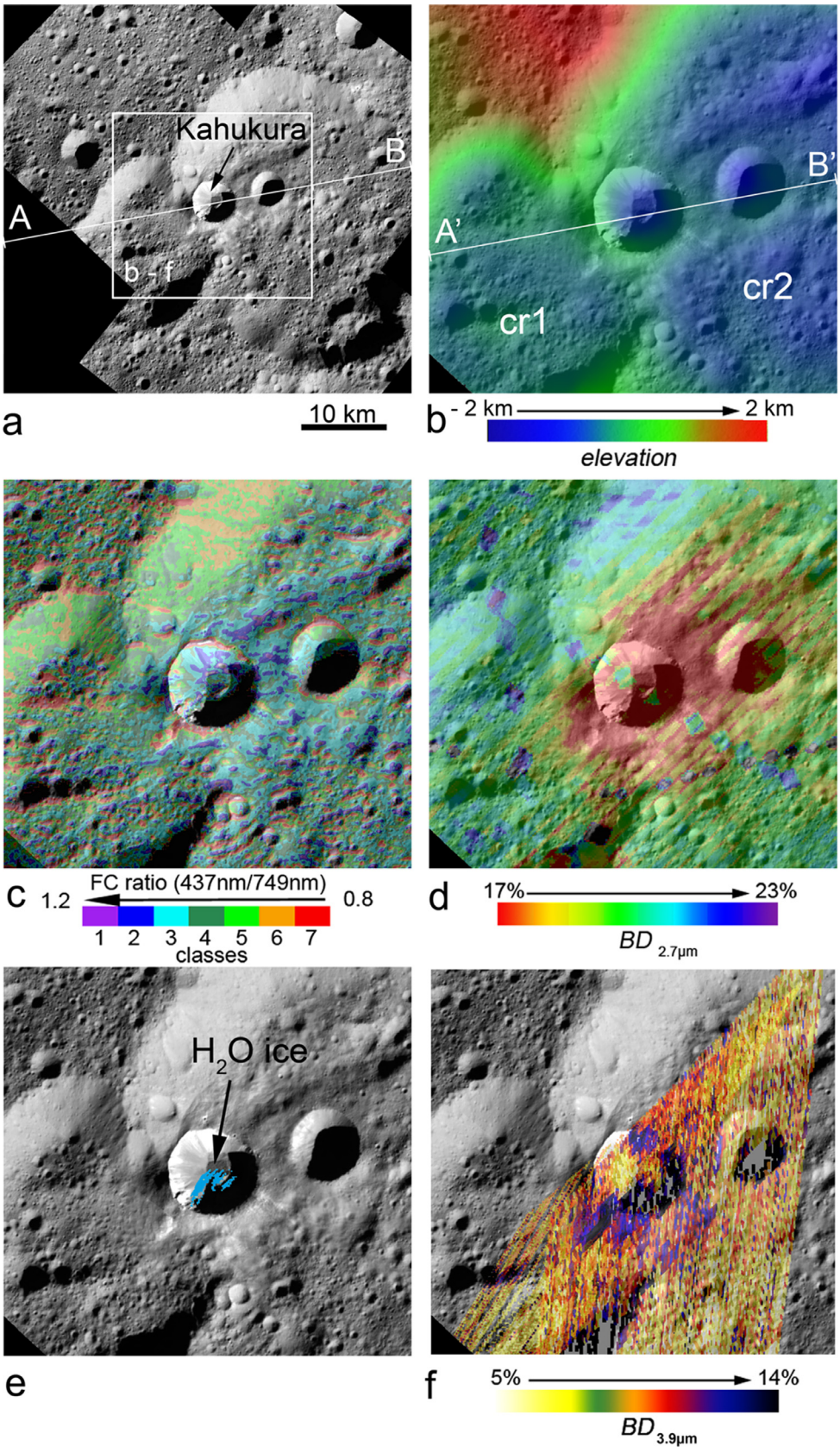

Fig. 11. Small fresh impact crater Kahukura and its location on the border of two larger geologically old impact craters (c1 and cr2) as seen in (a) the LAMO FC Clear filter mosaic in comparison to (b) the DTM, (c) the FC slope/ratio classes, the BDs of the absorptions at (d) 2.7 µm, (e) the location of H_2O ice deposits, as well as (f) the BD of the absorption at 3.9 µm derived for Kahukura (subset indicated by the white frame).

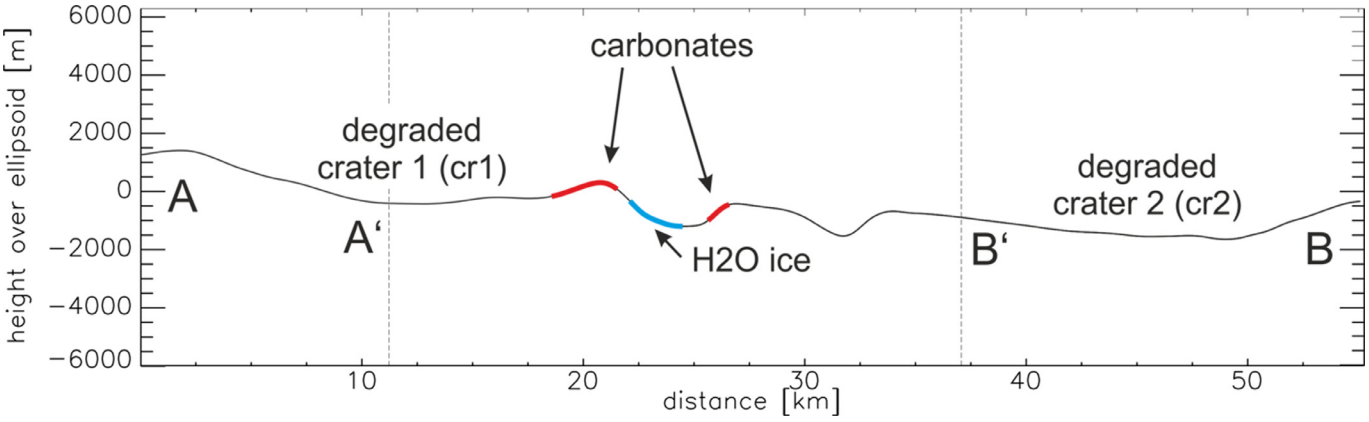

Fig. 12. Topographic profiles as indicated in Fig. 11 illustrating the location of Kahukura with respect to the geological context (Profile AB, Fig. 11a) and the close view onto Kahukura (Profile A'B', Fig. 11b–f) indicating the location of carbonate and H_2O ice deposits detected in the vicinity of the Kahukura (Fig. 11).

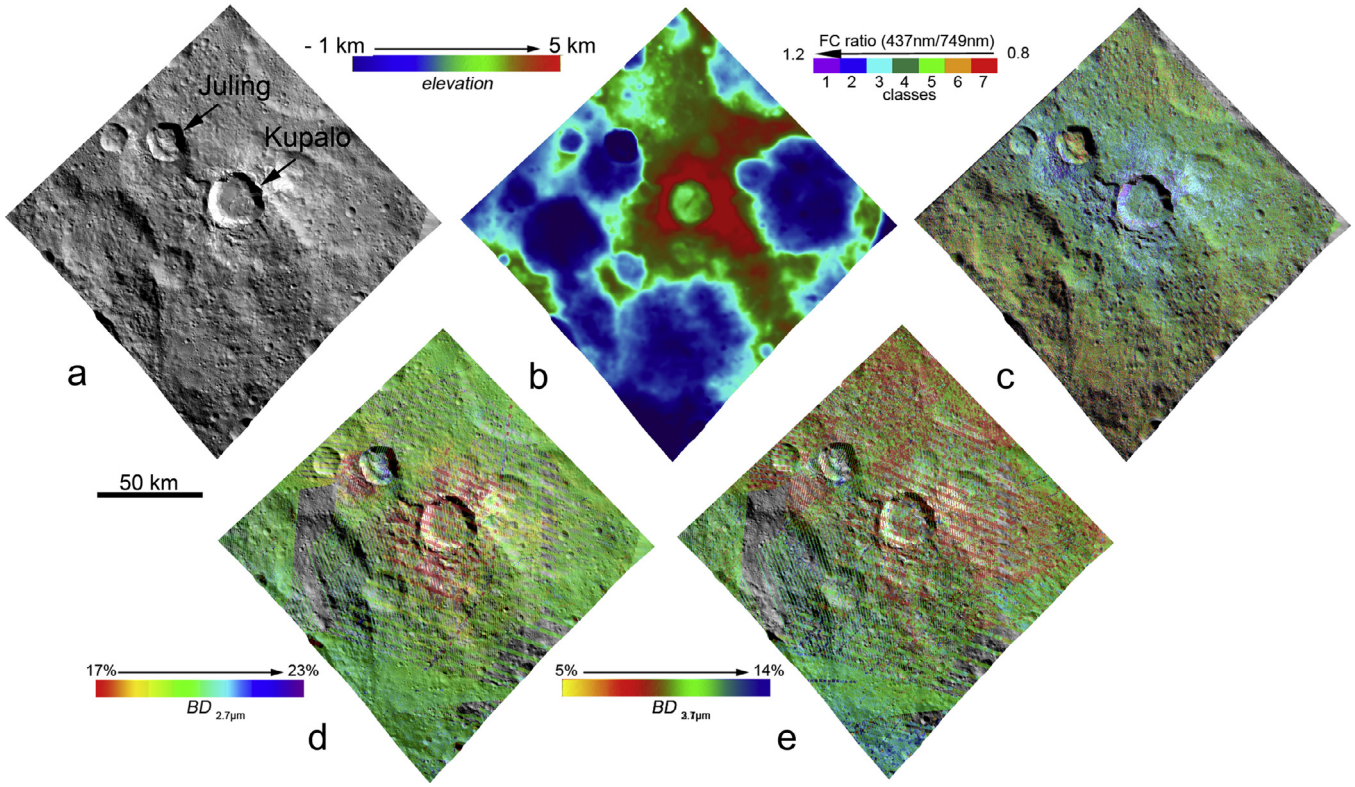

Fig. 13. Impact craters Kupalo and Juling as seen by (a) the LAMO FC Clear filter in comparison to (b) the corresponding DTM, (c) the FC slope/ratio classes as well as the band depths (*BD*) of the absorptions at (d) 2.7 and (e) 3.1 µm.

evident) or unconsolidated and geologically old weathered material. Thus, a red spectral slope in the Ceres' spectra can be caused by differences in the surface composition as well as the physical surface properties.

4. Discussion and evolution of Ceres surface

Our investigation of the relationships between the spectral and geological properties of individual impact craters reveals not only lateral heterogeneities in Ceres' surface composition and possible stratigraphical differences within Ceres' crust but also implies changes in the chemical or physical surface properties depending for how long the surface material has been exposed to space weathering. In order to check if the observed trends are valid for the entire Cerean surface, Fig. 14 compares the measured F8/F3 ratio and the BDs of the phyllosilicate absorptions of all Cerean impact craters with their absolute geological crater age derived during the Dawn geologic mapping campaign (Table 1). Absolute ages of numerous impact craters are available for both cratering models, the Lunar-derived Model Age (LDM) and/or the Asteroid Flux Model Age (AMA) (Hiesinger et al., 2016; Schmedemann et al., 2016).

It should be taken into account that the F8/F3 ratio and BD measurements also include effects of the specific crater size, pixel ground resolution and S/N-ratio influencing the accuracy of the measurements. Whereas for large craters a fairly 'pure' spectral signature can be derived, the spectral signature of small craters is more or less mixed with the one of the surroundings. Also a variable contribution of a dark presumably carbon-rich surface compound has not a major but certainly a small effect onto the measured F8/F3 ratio and the BD values. Despite these additional influences, distinct trends are recognizable in the graphs of Fig. 14, in-

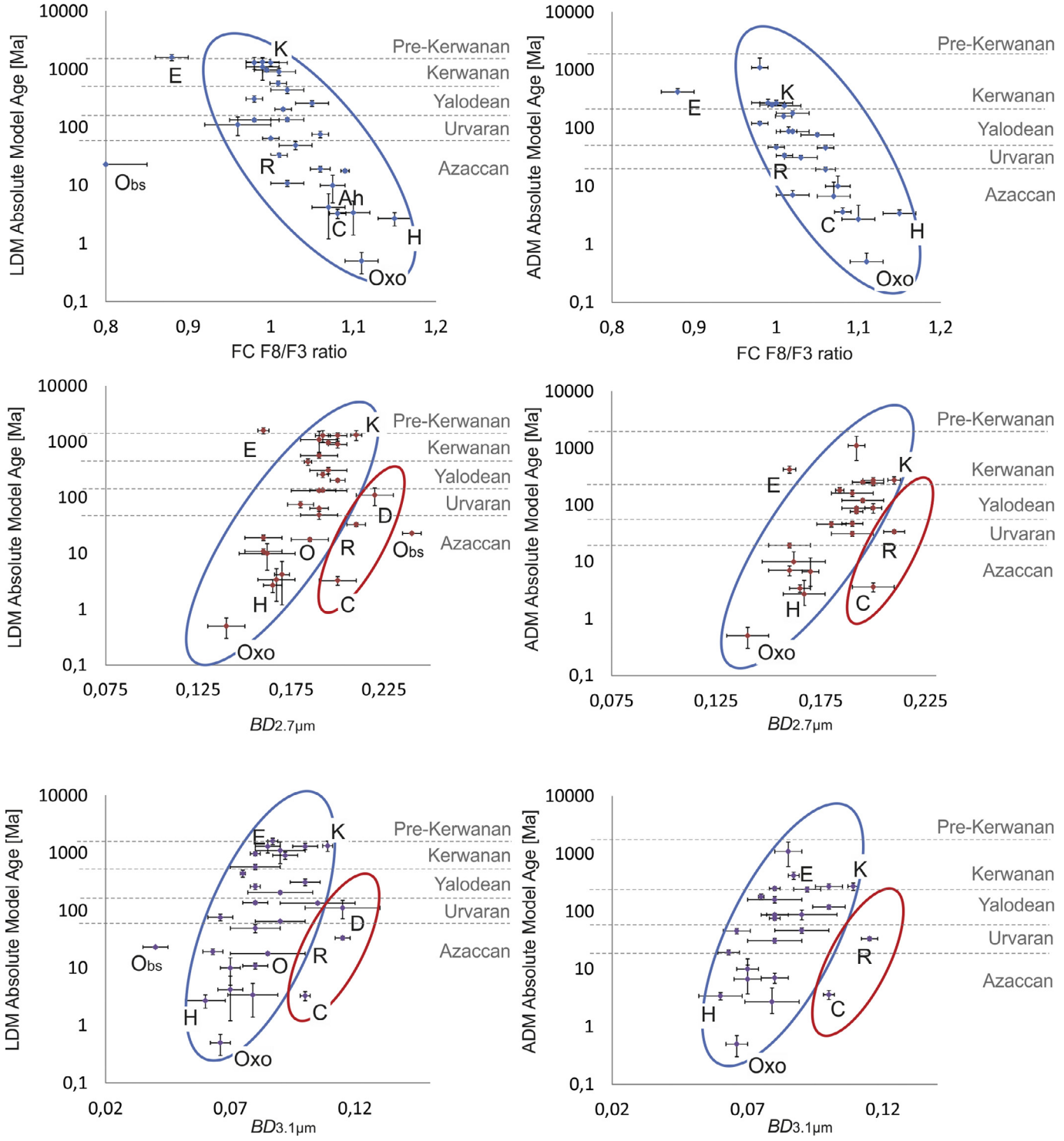

Fig. 14. Stratigraphic relationship between spectral properties and Cerean geological periods derived by the LDM (left column) and the ADM (right column). Type examples of impact craters: E – Ernutet, D – Dantu, R: Rao, C – Cacaguat, H – Haulani, O – Occator, O_{bs} – bright spots of Occator and Oxo (including the icy portion). Major trends are highlighted by the red and blue oval. (For interpretation of the references to color in this figure legend, the reader is referred to the web version of this article.)

dependent of which cratering model has been used. The F8/F3 ratio shows a distinct trend with a blue spectral slope in the vicinity of geologically young impact craters, which turns red with increasing geological age (framed by a blue oval). This bluing is apparently accompanied by a decreasing of the BDs at 2.7 and 3.1 µm. Intriguingly, the values measured for the potential cryovolcanic dome Ahuna Mons (Ah) discussed in detail in Ruesch et al. (2016) and Zambon et al. (2017) and the ice deposits of Oxo (Combe et al., 2016; Stephan et al., 2017a) also fit with this trend. However, few impact craters exhibit a different behavior (Fig. 14, framed by the red oval). The BD values at 2.7 and 3.1 µm of a few impact craters such as Dantu (D), the small young impact craters Rao (R, diameter: 12 km, 8.1°N/119.0°E) and Cacaguat (C, diameter: 13.6 km, 1.2°S/143.6°N) do not belong to the main cluster and exhibit distinctly deeper absorptions. These impact craters are all located within Ceres' large topographic low Vendimia Planitia (Fig. 2) with

Table 1
Diameter (D in km), geographic location, the spectral parameters derived in this work and the LDM and ADM crater model ages including the corresponding references of the crater model ages (Ref) of all impact craters included in Fig. 14. Given references (Ref.), which refer to both the LDM and ADM crater model ages, are Pa 17 - Pasckert et al. (2017), Sc16 – Schmedemann et al. (2016), Wi17 - Williams et al. (2017b), Wa17 - Wagner et al. (2017), Kn16 - Kneissl et al. (2016), Kr17 - Krohn et al. (2017), Hi16 - Hiesinger et al. (2016), Sz17 - Schulzeck et al. (2017), Cr17 - Crown et al. (2017), Sy17 – Scully et al. (2017), Ru16 - Ruesch et al. (2016), and Wa16 - Wagner et al. (2016).

Name	D/km	Location	F8/F3 ratio	BD 2.7μm	BD 3.1μm	LDM	ADM	Ref.
Achita	40	25.82°N/65.96°E	1.01±0.01	0.19±0.01	0.08±0.01	570±60	160±20	Pa17
Azacca	49.9	6.66°S/218.4°E	1.06±0.01	0.18±0.007	0.066±0.005	75.9±10	45.8±5	Sc16
Cacaguat	13.6	1,2°S/143,6°N	1.08±0.01	0.20±0.01	0.10±0.002	1.3±0.79	1.55±0.80	Wi17
Centeotl	6.0	18.9°N/141.2°E	1.07±0.02	0.17±0.004	0.07±0.005	4.2±3	6.7±4	Wa17
Coniraya	135	39.9°N/65.7°E	0.98±0.01	0.192±0.002	0.085±0.005	1300±300	1100±500	Pa17
Dantu	126	24.3°N/138.2°E	0.96±0.04	0.22±0.01	0.115±0.015	111±39	–	Kn16
Ernutet	53.4	52.9°N/45.5°E	0.88±0.02	0.16±0.003	0.087±0.002	1600±200	420±60	Pa17
Gaue	80	30.8°N/86.2°E	1.05±0.02	0.192±0.003	0.08±0.002	260±30	76±6	Pa17
Haulani	34	5.8°N/10.8°E	1.15±0.02	0.165±0.005	0.06±0.008	2.7±0.7	3.4±0.5	Kr17
Ikapati	50	33.8°N/45.6°E	1.06±0.012	0.16±0.01	0.063±0.004	19.2±2.2	19.4±1.9	Sc16
Kerwan	280	10.8°S/124°E	1.00±0.02	0.20±0.005	0.10±0.005	1300±160	281±17	Wi17
Liber	23	42.6°N/37.8°E	1.02±0.02	0.184±0.002	0.075±0.001	440±60	180±20	Pa17
Messor	40	49.9°N/233.7°E	1±0.01	0.19±0.005	0.09±0.01	64.5±2.6	46.8±4.9	Sc16
Occator (Obs)	92	19.8°N/239.3°E	1.09±0.005 (0.8±0.05)	0.185±0.01 (0.24±0.005)	0.085±0.015 (0.04±0.005)	17.8±1.2	–	Hi16
Omonga	77	58.0°N/71.7°E	0.995±0.015	0.195±0.005	0.08±0.002	970±70	250±20	Pa17
Oxo	10	42.2°N/359.6°E	1.11±0.02	0.14±0.01	0.66±0.004	0.5±0.2	0.5±0.2	Sc17
Rao	12	8.1°N/119.0°E	1.01±0.01	0.195±0.01	0.1±0.006	33.1±2.5	33.6±2.5	Wi17
Sintana	58	48.1°S/46.2°E	0.98±0.01	0.195±0.01	0.1±0.006	310±40	120±10	Sz17
Tupo	36	32.3°S/88.4°E	1.03±0.02	0.19±0.01	0.08±0.01	49±8	32±3	Sz17
Urvara	170	46.6°S/249.2°E	0.98±0.03	0.19±0.015	0.105±0.015	134±8	–	Cr17
Yalode	260	42.6°S/292.5°E	0.99±0.02	0.19±0.01	0.09±0.1	1100±450	–	Cr17
Kahukura	6	61.44°N/221.40°E	1.10±0.02	0.176±0,01	0.079±0.01	3.4±2	2.7±2	Wa17
Unnamed	24	62°N/253°E	1.02±0.02	0.16±0.01	0.08±0.005	10.9±1.3	7.04±1.4	Sy17
Unnamed	34	39°N/247°E	1.01±0.02	0.20±0.005	0.092±0.013	906±130	242±24	Sy17
Unnamed	15	23°N/186°E	1.015±0.01	0.20±0.004	0.09±0.013	205±12	88.1±17	Sy17
Unnamed	34	43.3°S/120.9°E	0.99±0.02	0.21±0.003	0.109±0.002	1330±270	272±41	Sc16
Ahuna Mons	20	10.3°S/316.5°E	1.075±0.015	0.162±0.0151	0.07±0.004	70±20/∼10	70±20/∼10	Ru16/Wa16

the measured BDs conform to the generally strong absorptions in the entire basin. Although the variations are small, decreasing the accuracy of the derived values, a similar trend is still visible when measuring the BDs of absorption at 3.1 μm and thus support the assumption of a higher abundance of ammoniated phyllosilicates in Vendemia Planitia. Although Kerwan (K) is also located within Vendimia Planitia, the BDs of the measured absorptions are smaller than observed for Dantu. Possibly Kerwan's original spectral properties are obscured or have been altered due to the ubiquitous superimposed younger surface features in this region. The spectral differences between the majority of investigated impact craters and Dantu, Rao and Cacaguat only occur with respect to the BD values. On the contrary, the F8/F3 ratio values of Dantu and its companions fit the general trend. Thus, two effects are visible here. The two main clusters of BD values are caused by compositional differences, whereas the decreasing of the BD values as well as the bluing of the spectral slope represent changes in Ceres' surface properties with time.

It has to be noted that the composition of all impact craters, whose ratio and BD values fit in one of these main cluster is dominated by phyllosilicates. On the contrary, the F8/F3 ratio values measured for the spectrally peculiar regions near the impact crater Ernutet (E) (De Sanctis et al., 2017a) and the carbonate-enriched spots on the floor of impact crater Occator (O_{bs}), which are discussed in detail by De Sanctis et al. (2016) and Longobardo et al. (2017) lie distinctly outside the main cluster (framed by the blue oval). Further, although, the average spectral properties of Occator (O) lie in the major trend, the bright spots within Occator (O_{bs}) exhibit the strongest absorption at 2.7 μm (BD of ∼24%) that can be measured on Ceres, but at the same time the weakest absorption at 3.1 μm (BD of ∼4%). This may be caused by the enrichment of this bright material in sodium carbonates and a depletion of phyllosilicates (Palomba et al., 2017b), which dominate the spectral properties of the rest of Ceres.

In summary, our measurements imply that a direct correlation between the bluing of the spectral slope indicated by the F8/F3 ratio and the geological surface age as predicted by Schmedemann et al. (2016) is valid, but is limited to portions of Ceres' surface that are dominated by phyllosilicates. A similar trend is also apparent in the BDs of the absorptions at 2.7 and 3.1 μm. However, variations in the BDs caused by different abundances of the phyllosilicates apparently do not influence the F8/F3 ratio. Further, a similarly blue slope has been observed for impact craters of different albedo and thus a possible varying contribution of dark carbon rich material. Thus the bluing of the spectral slope is unlikely due to a different surface composition, but is rather likely related to the physical properties of the phyllosilicates recently emplaced on Ceres' surface. Commonly, a spectral bluing is observed with increasing grain size of phyllosilicates (Cloutis et al., 2011; Cooper and Mustard, 1999). The blue spectral slope might also result from the impact events themselves due to grinding and melting of the Cerean surface material as discussed by Stephan et al. (2017a) and shown in laboratory experiments of Bishop et al. (2008). Relatively fine phyllosilicate grains easily melt (French, 1998) and form agglomerates during an impact, spectrally mimicking larger phyllosilicate grains (Cooper and Mustard, 1999). This theory is supported by Krohn et al. (2016), who observed an association of spectrally blue-sloped material with flow features of young impact craters and interpreted them as highly fluidized material/impact melt. A reddening of the spectral slope with increasing age can be explained by millions years of space weathering including solar insolation, micro-meteoritic bombardment and impacting cosmic rays resulting in an unconsolidated and fine-grained surface regolith. A reversal of the agglutination process could possible also be expected due to mass wasting processes such as slumping. Thus, the red spectral slope is mostly representative of Ceres' surface material, when it has been weathered over long geological periods. But it might, in some cases, alternatively indicate a particular particle size distribution or other physi-

cal properties characteristic of landslides due to the disintegration of crater wall material, or when it is consisted of material composed of material other than Ceres' average surface composition such as sodium carbonates and organics.

Because varying amounts of carbonates are existent in Ceres average surface composition (De Sanctis et al., 2015), it cannot be excluded completely at this point that a gradual mixing of phyllosilicates and carbonates as part of the weathering processes of Ceres' surface material contributes to the observed reddening of the spectral slope. Nevertheless, as seen in the vicinity of Occator, deposits enriched in carbonates only occur in spatially limited places and represent one of the youngest Cerean surface deposits (Palomba et al., 2017b). Geochemical models predict that carbonates as well as phyllosilicates have been formed by an extensive aqueous alteration (De Sanctis et al., 2015) either as a result of cryovolcanic (De Sanctis et al., 2016; Russell et al., 2016) or post-impact hydrothermal activity (Bowling et al., 2016).

References

Ammannito, E., De Sanctis, M.C., Carrozzo, F.G., Zambon, F., Ciarniello, M., Combe, J.-P., Frigeri, A., Longobardo, A., Raponi, A., Fonte, S., Giardino, M., Hughson, K., McFadden, L.A., Palomba, E., Scully, J., Stephan, K., Raymond, C.A., Russell, C.T., 2017. Composition of the Urvara-Yalode region on Ceres. Lunar and Planetary Science Conference, Volume 48 abstract # 2659.

Ammannito, E., DeSanctis, M.C., Ciarniello, M., Frigeri, A., Carrozzo, F.G., Combe, J.-P., Ehlmann, B.L., Marchi, S., McSween, H.Y., Raponi, A., Toplis, M.J., Tosi, F., Castillo-Rogez, J.C., Capaccioni, F., Capria, M.T., Fonte, S., Giardino, M., Jaumann, R., Longobardo, A., Joy, S.P., Magni, G., McCord, T.B., McFadden, L.A., Palomba, E., Pieters, C.M., Polanskey, C.A., Rayman, M.D., Raymond, C.A., Schenk, P.M., Zambon, F., Russell, C.T., 2016. Distribution of phyllosilicates on the surface of Ceres. Science 353 (6303), aaf4279.

Bishop, J.L., Dyar, M.D., Sklute, E.C., Drief, A., 2008. Physical alteration of antigorite: a Mössbauer spectroscopy, reflectance spectroscopy and TEM study with applications to Mars. Clay Miner. 43 (1), 55–67.

Bowling, T.J., Ciesla, F.J., Marchi, S., Davison, T.M., Castillo-Rogez, J.C., De Sanctis, M.C., Raymond, C.A., Russell, C.T., 2016. Impact induced heating of Occator crater on Asteroid 1 Ceres. Lunar and Planetary Science Conference, Volume 47 abstract # 2268.

Buczkowski, D.L., Schmidt, B.E., Williams, D.A., Mest, S.C., Scully, J.E.C., Ermakov, A.I., Preusker, F., Schenk, P., Otto, K.A., Hiesinger, H., O'Brien, D., Marchi, S., Sizemore, H., Hughson, K., Chilton, H., Bland, M., Byrne, S., Schorghofer, N., Platz, T., Jaumann, R., Roatsch, T., Sykes, M.V., Nathues, A., De Sanctis, M.C., Raymond, C.A., Russell, C.T., 2016. The geomorphology of Ceres. Science 353 (6303), aaf4332.

Buczkowski, D.L., Williams, D.A., Scully, J.E.C., Mest, S.C., Crown, D.A., Schenk, P.M., Jaumann, R., Roatsch, T., Preusker, F., Platz, T., Nathues, A., Hoffmann, M., Schaefer, M., Marchi, S., De Sanctis, M.C., Raymond, C.A., Russell, C.T., 2017. The geology of the occator quadrangle of dwarf planet Ceres: floor-fractured craters and other geomorphic evidence of cryomagmatism. Icarus https://doi.org/10.1016/j.icarus.2017.05.025.

Cahill, J.T.S., Lucey, P.G., Wieczorek, M.A., 2009. Compositional variations of the lunar crust: results from radiative transfer modeling of central peak spectra. J. Geophys. Res. 114 (E9). doi:10.1029/2008JE003282.

Carrozzo, F.G., Raponi, A., Sanctis, M.C.D., Ammannito, E., Giardino, M., D'Aversa, E., Fonte, S., Tosi, F., 2016. Artifacts reduction in VIR/Dawn data. Rev. Sci. Instrum. 87 (12), 124501.

Ciarniello, M., De Sanctis, M.C., Ammannito, E., Raponi, A., Longobardo, A., Palomba, E., Carrozzo, F.G., Tosi, F., Li, J.-Y., Schröder, S.E., Zambon, F., Frigeri, A., Fonte, S., Giardino, M., Pieters, C.M., Raymond, C.A., and Russell, C.T., 2016, Spectrophotometric properties of dwarf planet Ceres from the VIR spectrometer on board the Dawn mission, ArXiv e-prints, Volume 1608.

Cloutis, E.A., Hiroi, T., Gaffey, M.J., Alexander, C.M.O.D., Mann, P., 2011. Spectral reflectance properties of carbonaceous chondrites: 1. CI chondrites. Icarus 212 (1), 180–209.

Combe, J.-P., McCord, T.B., Tosi, F., Ammannito, E., Carrozzo, F.G., De Sanctis, M.C., Raponi, A., Byrne, S., Landis, M.E., Hughson, K.H.G., Raymond, C.A., Russell, C.T., 2016. Detection of local H2O exposed at the surface of Ceres. Science 353. doi:10.1126/science.aaf3010.

Combe, J.-P., Raponi, A., Tosi, F., De Sanctis, M.-C., Ammannito, E., Carrozzo, F.G., Landis, M.E., Byrne, S., Carsenty, U., Schröder, S., Platz, T., Ruesch, O., Hughson, K.H.G., MCCord, T.B., Singh, S., Johnson, K.E., Zambon, F., Pieters, C.M., Raymond, C.A., Russell, C.T., 2017. Exposed H2O-rich areas on Ceres detected by Dawn. Lunar and Planetary Science Conference, Volume 48.

Cooper, C.D., Mustard, J.F., 1999. Effects of very fine particle size on reflectance spectra of smectite and palagonitic soil. Icarus 142, 557–570.

Crown, D.A., Sizemore, H.G., Yingst, R.A., Mest, S.C., Platz, T., Berman, D.C., Schmedemann, N., Buczkowski, D.L., Williams, D.A., Roatsch, T., Preusker, F., Raymond, C.A., Russell, C.T., Geologic mapping of the Urvara and Yalode Quadrangles of Ceres, Icarus, https://doi.org/10.1016/j.icarus.2017.08.004.

De Sanctis, M.C., Ammannito, E., McSween, H.Y., Raponi, A., Marchi, S., Capaccioni, F., Capria, M.T., Carrozzo, F.G., Ciarniello, M., Fonte, S., Formisano, M., Frigeri, A., Giardino, M., Longobardo, A., Magni, G., McFadden, L.A., Palomba, E., Pieters, C.M., Tosi, F., Zambon, F., Raymond, C.A., Russell, C.T., 2017a. Localized aliphatic organic material on the surface of Ceres. Science 355, 719–722.

De Sanctis, M.C., Ammannito, E., Raponi, A., Marchi, S., McCord, T.B., McSween, H.Y., Capaccioni, F., Capria, M.T., Carrozzo, F.G., Ciarniello, M., Longobardo, A., Tosi, F., Fonte, S., Formisano, M., Frigeri, A., Giardino, M., Magni, G., Palomba, E., Turrini, D., Zambon, F., Combe, J.-P., Feldman, W., Jaumann, R., McFadden, L.A., Pieters, C.M., Prettyman, T., Toplis, M., Raymond, C.A., Russell, C.T., 2015. Ammoniated phyllosilicates with a likely outer Solar System origin on (1) Ceres. Nature 528, 241–244.

De Sanctis, M.C., Coradini, A., Ammannito, E., Filacchione, G., Capria, M.T., Fonte, S., Magni, G., Barbis, A., Bini, A., Dami, M., Ficai-Veltroni, I., Preti, G., 2011. The VIR spectrometer. Space Sci. Rev. 163, 329–369.

De Sanctis, M.C., Frigeri, A., Ammannito, E., Carrozzo, F.G., Ciarniello, M., Zambon, F., Tosi, F., Raponi, A., Longobardo, A., Combe, J.P., Palomba, E., Schulzeck, F., Raymond, C.A., Russell, C.T., 2017b. Ac-H-11 Sintana and Ac-H-12 Toharu quadrangles: assessing the large and small scale heterogeneities of Ceres' surface. Icarus.

De Sanctis, M.C., Raponi, A., Ammannito, E., Ciarniello, M., Toplis, M.J., McSween, H.Y., Castillo-Rogez, J.C., Ehlmann, B.L., Carrozzo, F.G., Marchi, S., Tosi, F., Zambon, F., Capaccioni, F., Capria, M.T., Fonte, S., Formisano, M., Frigeri, A., Giardino, M., Longobardo, A., Magni, G., Palomba, E., McFadden, L.A., Pieters, C.M., Jaumann, R., Schenk, P., Mugnuolo, R., Raymond, C.A., Russell, C.T., 2016. Bright carbonate deposits as evidence of aqueous alteration on (1) Ceres. Nature 536, 54–57.

Ermakov, A.I., Park, R.S., Zuber, M.T., Smith, D.E., Fu, R.R., Sori, M.M., Raymond, C.A., Russell, C.T., 2017. Regional analysis of Ceres' gravity anomalies. Lunar and Planetary Science Conference, Volume 48.

French, B.M., 1998. Traces of Catastrophe: A Handbook of Shock-Metamorphic Effects in Terrestrial Meteorite Impact Structures. LPI-Contrib-954 Technical Report.

Fu, R.R., Ermakov, A.I., Marchi, S., Castillo-Rogez, J.C., Raymond, C.A., Hager, B.H., Zuber, M.T., King, S.D., Bland, M.T., Cristina De Sanctis, M., Preusker, F., Park, R.S., Russell, C.T., 2017. The interior structure of Ceres as revealed by surface topography. Earth Planet. Sci. Lett. 476, 153–164.

Hiesinger, H., Marchi, S., Schmedemann, N., Schenk, P., Pasckert, J.H., Neesemann, A., O'Brien, D.P., Kneissl, T., Ermakov, A.I., Fu, R.R., Bland, M.T., Nathues, A., Platz, T., Williams, D.A., Jaumann, R., Castillo-Rogez, J.C., Ruesch, O., Schmidt, B., Park, R.S., Preusker, F., Buczkowski, D.L., Russell, C.T., Raymond, C.A., 2016. Cratering on Ceres: implications for its crust and evolution. Science 353 (6303), aaf4759.

Jaumann, R., Stephan, K., Krohn, K., Matz, K.-D., Otto, K., Neumann, W., Kneissl, T., Schmedemann, N., Schroeder, S., Tosi, F., De Sanctis, M.C., Preusker, F., Buczkowski, D., Capaccioni, F., Carsenty, U., Elgner, S., von der Gathen, I., Gieber, T., Hiesinger, H., Hoffmann, M., Kersten, E., Li, J.-Y., McCord, T.B., McFadden, L., Mottola, S., Nathues, A., Neesemann, A., Raymond, C., Roatsch, T., Russell, C.T., Schmidt, B., Schulzeck, F., Wagner, R., Williams, D.A., 2016. Age-dependent morphological and compositional variations on Ceres. Lunar and Planetary Science Conference, Volume 47 abstract # 1455.

Kneissl, T., Schmedemann, N., Neesemann, A., Williams, D.A., Crown, D.A., Mest, S.C., Buczkowski, D.L., Scully, J.E.C., Frigeri, A., Ruesch, O., Hiesinger, H., Walter, S.H.G., Jaumann, R., Roatsch, T., Preusker, F., Kersten, E., Nass, A., Nathues, A., Platz, T., Hoffmann, M., Schaefer, M., De Sanctis, M.C., Raymond, C.A., Russell, C.T., 2016. Geologic mapping of the Ac-H-3 Dantu quadrangle of Ceres from NASA's Dawn mission. Lunar and Planetary Science Conference, Volume 47 abstract # 1967.

Krohn, K., Jaumann, R., Stephan, K., Otto, K.A., Schmedemann, N., Wagner, R.J., Matz, K.D., Tosi, F., Zambon, F., von der Gathen, I., Schulzeck, F., Schröder, S.E., Buczkowski, D.L., Hiesinger, H., McSween, H.Y., Pieters, C.M., Preusker, F., Roatsch, T., Raymond, C.A., Russell, C.T., Williams, D.A., 2016. Cryogenic flow features on Ceres: implications for crater-related cryovolcanism. Geophys. Res. Lett. 43 (23) 11,994–912,003.

Krohn, K., Jaumann, R., Otto, K.A., Schulzeck, F., Neesemann, A., Nass, A., Stephan, K., Tosi, F., Wagner, R.J., Zambon, F., von der Gathen, I., Williams, D.A., Buczkowski, D.L., De Sanctis, M.C., Kersten, E., Matz, K.-D., Mest, S.C., Pieters, C.M., Preusker, F., Roatsch, T., Scully, J.E.C., Russell, C.T., Raymond, C.A., 2017. The unique geomorphology and structural geology of the Haulani crater of dwarf planet Ceres as revealed by geological mapping of the equatorial quadrangle Ac-6 Haulani. Icarus https://doi.org/10.1016/j.icarus.2017.09.014.

Longobardo, A., Palomba, E., Carrozzo, F.G., Galiano, A., De Sanctis, M.C., Stephan, K., Tosi, F., Raponi, A., Ciarniello, M., Zambon, F., Frigeri, A., Ammannito, E., Raymond, C.A., Russell, C.T., 2017. Mineralogy of the Occator quadrangle. Icarus https://doi.org/10.1016/j.icarus.2017.09.022.

Marchi, S., Ermakov, A.I., Raymond, C.A., Fu, R.R., O'Brien, D.P., Bland, M.T., Ammannito, E., de Sanctis, M.C., Bowling, T., Schenk, P., Scully, J.E.C., Buczkowski, D.L., Williams, D.A., Hiesinger, H., Russell, C.T., 2016. The missing large impact craters on Ceres. Nat. Commun. 7.

McCord, T.B., Zambon, F., 2017. The surface composition of Ceres from the Dawn mission. Icarus submitted.

Melosh, H.J., 1989. Impact Cratering: A Geologic Process. Oxford University Press, New York.

Melosh, H.J., 2011. Planetary Surface Processes. Cambridge University Press, Cambridge, U. K. Cambridge Planetary Science Series.

Mest, S.C., Crown, D.A., Yingst, R.A., Berman, D.C., Williams, D.A., Buczkowski, D.L., Scully, J.E.C., Platz, T., Jaumann, R., Preusker, F., Nathues, A., Hiesinger, H., Pasckert, J.H., Raymond, C.A., Russell, C.T., Team, D.S., 2017. The global geologic map

of Ceres based on Dawn HAMO observations. Lunar and Planetary Science Conference, Volume 48.

Palomba, E., Longobardo, A., De Sanctis, M.C., Carrozzo, F.G., Galiano, A., Zambon, F., Raponi, A., Ciarniello, M., Stephan, K., Williams, D.A., Ammannito, E., Capria, M.T., Fonte, S., Giardino, M., Tosi, F., Raymond, C.A., Russell, C.T., 2017a. Mineralogical mapping of the Kerwan quadrangle on Ceres. Icarus https://doi.org/10.1016/j.icarus.2017.07.021.

Palomba, E., Longobardo, A., De Sanctis, M.C., Stein, N.T., Ehlmann, B., Galiano, A., Raponi, A., Ciarniello, M., Ammannito, E., Cloutis, E., Carrozzo, F.G., Capria, M.T., Stephan, K., Zambon, F., Tosi, F., Raymond, C.A., Russell, C.T., 2017b. Compositional differences among bright spots on the Ceres surface. Icarus https://doi.org/10.1016/j.icarus.2017.09.020.

Park, R.S., Konopliv, A.S., Bills, B.G., Rambaux, N., Castillo-Rogez, J.C., Raymond, C.A., Vaughan, A.T., Ermakov, A.I., Zuber, M.T., Fu, R.R., Toplis, M.J., Russell, C.T., Nathues, A., Preusker, F., 2016. A partially differentiated interior for (1) Ceres deduced from its gravity field and shape. Nature 537 (7621), 515–517.

Pasckert, J.H., Hiesinger, H., Ruesch, O., Williams, D.A., Nass, A., Kneissl, T., Mest, S.C., Buczkowski, D.L., Scully, J.E.C., Schmedemann, N., Jaumann, R., Roatsch, T., Preusker, F., Nathues, A., Hoffmann, M., Schäfer, M., De Sanctis, M.C., Raymond, C.A., Russell, C.T., 2017. Geologic mapping of the Ac-2 Coniraya quadrangle of Ceres from NASA's Dawn mission: Implications for a heterogeneously composed crust. Icarus https://doi.org/10.1016/j.icarus.2017.06.015.

Pieters, C.M., Ammannito, E., Ciarniello, M., De Sanctis, M.C., Hoffman, M., Jaumann, R., McCord, T.B., McFadden, L.A., Mest, S., Nathues, A., Raponi, A., Raymond, C.A., Russell, C.T., Schaefer, M., Schenk, P., 2016. Surface processes and space weathering on Ceres. Lunar and Planetary Science Conference, Volume 47 abstract # 1383.

Platz, T., Nathues, A., Schorghofer, N., Preusker, F., Mazarico, E., Schröder, S.E., Byrne, S., Kneissl, T., Schmedemann, N., Combe, J.-P., Schäfer, M., Thangjam, G.S., Hoffmann, M., Gutierrez-Marques, P., Landis, M.E., Dietrich, W., Ripken, J., Matz, K.-D., Russell, C.T., 2016. Surface water-ice deposits in the northern shadowed regions of Ceres. Nature Astron. 1.

Prettyman, T.H., Feldman, W.C., McSween, H.Y., Dingler, R.D., Enemark, D.C., Patrick, D.E., Storms, S.A., Hendricks, J.S., Morgenthaler, J.P., Pitman, K.M., Reedy, R.C., 2011. Dawn's gamma ray and neutron detector. Space Sci. Rev. 163, 371–459.

Prettyman, T.H., Yamashita, N., Toplis, M.J., McSween, H.Y., Schörghofer, N., Marchi, S., Feldman, W.C., Castillo-Rogez, J., Forni, O., Lawrence, D.J., Ammannito, E., Ehlmann, B.L., Sizemore, H.G., Joy, S.P., Polanskey, C.A., Rayman, M.D., Raymond, C.A., Russell, C.T., 2017. Extensive water ice within Ceres' aqueously altered regolith: evidence from nuclear spectroscopy. Science 355 (6320), 55–59.

Preusker, F., Scholten, F., Matz, K.-D., Elgner, S., Jaumann, R., Roatsch, T., Joy, S.P., Polanskey, C.A., Raymond, C.A., Russell, C.T., 2016. Dawn at Ceres — shape model and rotational state. Lunar and Planetary Science Conference, Volume 47 abstract # 1954.

Raponi, A., De Sanctis, M.C., Ciarniello, M., Ammannito, E., Frigeri, A., Combe, J.-P., Tosi, F., Zambon, F., Carrozzo, F.G., Magni, G., Capria, M.T., Formisano, M., Longobardo, A., Palomba, E., Pieters, C.M., Russell, C.T., Raymond, C.A., 2017a. Water ice on Ceres' surface as seen by Dawn-Vir: properties retrieval by means of spectral modeling. Lunar and Planetary Science Conference, Volume 48 abstract # 2007.

Raponi, A., Carrozzo, F.C., Zambon, F., De Sanctis, M.C., Ciarniello, M., Frigeri, A., Ammannito, E., Tosi, F., Combe, J.-Ph., Longobardo, A., Palomba, E., Pieters, C.M., Raymond, C.A., Russell, C.T., Mineralogical mapping of Coniraya quadrangle of the dwarf planet Ceres, Icarus, https://doi.org/10.1016/j.icarus.2017.10.023.

Raymond, C.A., Castillo-Rogez, J.C., Ermakov, A., Park, R.S., Marchi, S., Bland, M.T., Fu, R.R., Mitri, G., Ammannito, E., De Sanctis, M.C., Toplis, M.J., Prettyman, T.H., Russell, C.T., 2017. Large-scale heterogeneity of Ceres: clues to interior evolution. Lunar and Planetary Science Conference, Volume 48.

Roatsch, T., Kersten, E., Matz, K.-D., Preusker, F., Scholten, F., Jaumann, R., Raymond, C.A., Russell, C.T., 2016. High-resolution Ceres high altitude mapping orbit atlas derived from Dawn Framing Camera images. Planet. Space Sci. 129, 103–107.

Ruesch, O., Platz, T., Schenk, P., McFadden, L.A., Castillo-Rogez, J.C., Quick, L.C., Byrne, S., Preusker, F., O'Brien, D.P., Schmedemann, N., Williams, D.A., Li, J.-Y., Bland, M.T., Hiesinger, H., Kneissl, T., Neesemann, A., Schaefer, M., Pasckert, J.H., Schmidt, B.E., Buczkowski, D.L., Sykes, M.V., Nathues, A., Roatsch, T., Hoffmann, M., Raymond, C.A., Russell, C.T., 2016. Cryovolcanism on Ceres. Science 353 (6303), aaf4286.

Russell, C.T., Raymond, C.A., Ammannito, E., Buczkowski, D.L., De Sanctis, M.C., Hiesinger, H., Jaumann, R., Konopliv, A.S., McSween, H.Y., Nathues, A., Park, R.S., Pieters, C.M., Prettyman, T.H., McCord, T.B., McFadden, L.A., Mottola, S., Zuber, M.T., Joy, S.P., Polanskey, C., Rayman, M.D., Castillo-Rogez, J.C., Chi, P.J., Combe, J.P., Ermakov, A., Fu, R.R., Hoffmann, M., Jia, Y.D., King, S.D., Lawrence, D.J., Li, J.-Y., Marchi, S., Preusker, F., Roatsch, T., Ruesch, O., Schenk, P., Villarreal, M.N., Yamashita, N., 2016. Dawn arrives at Ceres: exploration of a small, volatile-rich world. Science 353 (6303), 1008–1010.

Schenk, P.M., Buczkowski, D., Scully, J.E.C., De Sanctis, M.C., Schmidt, B.E., O'Brien, D.P., Hiesinger, H., Sizemore, H.G., Ammannito, E., Raymond, C., Russell, C.T., Team, D.S., 2016. Central pit and dome formation as seen in Occator crater, Ceres. AAS/Division for Planetary Sciences Meeting Abstracts, Volume 48 abstract # 2697.

Schmedemann, N., Kneissl, T., Neesemann, A., Stephan, K., Jaumann, R., Krohn, K., Michael, G.G., Matz, K.D., Otto, K.A., Raymond, C.A., Russell, C.T., 2016. Timing of optical maturation of recently exposed material on Ceres. Geophys. Res. Lett. 43 (23) 11,987–911,993.

Sierks, H., Keller, H.U., Jaumann, R., Michalik, H., Behnke, T., Bubenhagen, F., Büttner, I., Carsenty, U., Christensen, U., Enge, R., Fiethe, B., Gutiérrez Marqués, P., Hartwig, H., Krüger, H., Kühne, W., Maue, T., Mottola, S., Nathues, A., Reiche, K.-U., Richards, M.L., Roatsch, T., Schröder, S.E., Szemerey, I., Tschentscher, M., 2011. The Dawn Framing Camera. Space Sci. Rev. 163, 263–327.

Stephan, K., Jaumann, R., Krohn, K., Schmedemann, N., Zambon, F., Tosi, F., Carrozzo, F.G., McFadden, L.A., Otto, K., De Sanctis, M.C., Ammannito, E., Matz, K.D., Roatsch, T., Preusker, F., Raymond, C.A., Russell, C.T., 2017a. An investigation of the bluish material on Ceres. Geophys. Res. Lett. 44 (4), 1660–1668.

Stephan, K., Jaumann, R., Zambon, F., Carrozzo, F.G., De Sanctis, M.C., Tosi, F., Longobardo, A., Palomba, E., Ammannito, E., McFadden, L.A., Krohn, K., Williams, D.A., Raponi, A., Ciarnello, M., Combe, J.P., Frigeri, A., Roatsch, T., Matz, K.D., Preusker, F., Raymond, C.A., Russell, C.T., 2017b. Spectral investigation of quadrangle AC-H 3 of the dwarf planet Ceres – the region of impact crater Dantu. Icarus doi:10.1016/j.icarus.2017.07.019.

Tosi, F., Carrozzo, F.C., Zambon, F., Ciarniello, M., Frigeri, A., Combe, J.-Ph., De Sanctis, M.C., Hoffmann, M., Longobardo, A., Nathues, A., Raponi, A., Thangjam, G., Ammannito, E., Krohn, K., McFadden, L.A., Palomba, E., Pieters, C.M., Stephan, K., Raymond, C.A., Russell, C. T., 2017. The Dawn Science Team, Minerolgical analysis of the Ac-H-6 Haulani quadrangle of dwarf planet Ceres https://doi.org/10.1016/j.icarus.2017.08.012.

Wagner, R.J., Schmedemann, N., Stephan, K., Jaumann, R., Kneissl, T., Neesemann, A., Krohn, K., Otto, K., Preusker, F., Kersten, E., Roatsch, T., Hiesinger, H., Williams, D.A., Yingst, R.A., Crown, D.A., Mest, S.C., Raymond, C.A., Russell, C.T., 2016. Stratigraphy of (1) Ceres from geologic and topographic mapping and crater counts using images of the Dawn FC2 camera. Lunar and Planetary Science Conference, Volume 47 abstract # 2156.

Wagner, R.J., Schmedemann, N., Stephan, K., Jaumann, R., Neesemann, A., Krohn, K., Otto, K., Preusker, F., Kersten, E., Roatsch, T., Hiesinger, H., Williams, D.A., Aileen Yingst, R., Crown, D.A., Mest, S.C., Raymond, C.A., Russell, C.T., 2017. Geologic evolution of the dwarf planet (1) Ceres: results from geologic mapping using Dawn FC2 camera imaging data and an update in cratering model ages. In: EGU General Assembly Conference Abstracts, Volume 19, p. 13748.

Wieczorek, M.A., Zuber, M.T., 2001. The composition and origin of the lunar crust: constraints from central peaks and crustal thickness modeling. Geophys. Res. Lett. 28 (21), 4023–4026.

Williams, D.A., Buczkowski, D.L., Mest, S.C., Scully, J.E.C., Platz, T., Kneissl, T., 2017a. Introduction: the geologic mapping of Ceres. Icarus https://doi.org/10.1016/j.icarus.2017.05.004.

Williams, D.A., Kneissl, T., Neesemann, A., Mest, S.C., Palomba, E., Platz, T., Nathues, A., Longobrado, A., Scully, J.E.C., Ermakov, A., Jaumann, R., Buczkowski, D.L., Schäfer, M., Thangjam, G., Pieters, C.M., Roatsch, T., Preusker, F., Marchi, S., Schmedemann, N., Hiesinger, H., Frigeri, A., Raymond, C.A., Russell, C.T., 2017b. The geology of the Kerwan quadrangle of dwarf planet Ceres: Investigating Ceres' oldest, largest impact basin. Icarus https://doi.org/10.1016/j.icarus.2017.08.015.

Zahnle, K., Schenk, P., Levison, H., Dones, L., 2003. Cratering rates in the outer solar system. Icarus 163, 263–289.

Zambon, F., Raponi, A., Tosi, F., De Sanctis, M.C., McFadden, L.A., Carrozzo, F.G., Longobardo, A., Ciarniello, M., Krohn, K., Stephan, K., Palomba, E., Pieters, C.M., Ammannito, E., Russell, C.T., Raymond, C.A., 2017. Spectral analysis of Ahuna Mons from Dawn mission's visible-infrared spectrometer. Geophys. Res. Lett. 44, 97–104.

Zolotov, M.Y., 2017. Aqueous origins of bright salt deposits on Ceres. Icarus 296, 289–304.